Modelling and Analysis of Center of Pressure Data

by

Adam Webber
B.Sc., Dalhousie University, 2001

A Thesis Submitted in Partial Fulfillment of the
Requirements for the Degree of

MASTERS OF SCIENCE

in the Department of Mathematics and Statistics

We accept this thesis as conforming
to the required standard

[redacted]

Dr. M. Lesperance, Supervisor (Department of Mathematics & Statistics)

[redacted]

Dr. R. Edwards, Supervisor (Department of Mathematics & Statistics)

[redacted]

Dr. N Virji-Babul, Outside Member (Department of Psychology)

[redacted]

Dr. E. Paul Zehr, External Examiner (School of Physical Education)

Supervisors: Dr. M. Lesperance and Dr. R. Edwards
(Department of Mathematics and Statistics)

Abstract

Center of Pressure (COP) data has been used in the study of postural control for several decades. This study has usually been limited to basic measures of the COP trajectory, such as velocity. In the last decade, attempts have been made to extract more meaningful physiological parameters through the use of mathematical modelling of the postural control system. Beginning with stabilogram-diffusion analysis and focusing on the Pinned Polymer, Inverted Pendulum and FARIMA models of quiet stance, this thesis reviews some of the attempts get physiological estimates from COP data, and applies the three models to a subject group consisting of Down syndrome and non-Down syndrome individuals. These models have not previously been applied to Down syndrome subjects. The resulting estimates from each model are examined, and the strengths and weaknesses of each are discussed, as well as possibilities for future work.

Examiners:

[redacted]

Dr. M. Lesperance, Supervisor (Department of Mathematics & Statistics)

[redacted]

Dr. R. Edwards, Supervisor (Department of Mathematics & Statistics)

[redacted]

Dr. N Virji-Babul, Outside Member (Department of Psychology)

[redacted]

Dr. E. Paul Zehr, External Examiner (School of Physical Education)

Contents

List of Figures

Chapter 1

Introduction

Maintaining an upright stance is a surprisingly complex physiological task. Research has shown that three main systems are called upon during postural control; somatosensory, vestibular and visual (Shumway-Cook and Woollacott, 2000). While the individual functions of each system are well known, they interact in many different ways, not all of which are well understood. In patients with balance control problems this can make it difficult to diagnose the system(s) in which the problems lie. A more accurate description of the nature of a patients' problems should lead to more effective treatments. Several attempts at modelling the postural system, presented here, do not distinguish between the various input systems, but have been developed to take easily obtainable patient data such as a COP trajectory and derive useful physiological information from them.

Centre of Pressure (COP) trajectories are often collected on patients during simple tasks, such as standing. A COP trajectory consists of a series of

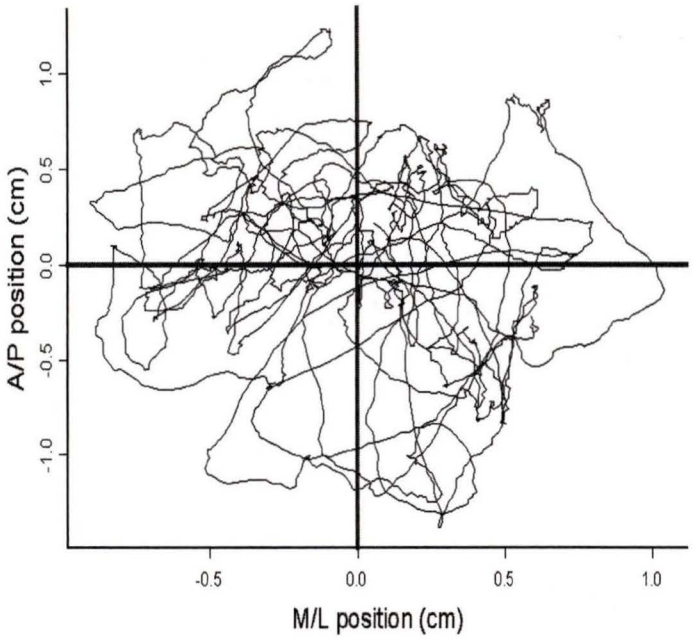

Figure 1.1: A "typical" Center of Pressure (COP) trajectory. A COP trajectory shows the movement of a subject's COP over the course of a 30 s trial.

points in the (x, y)-plane which track a subject's centre of pressure over time (see Figure 1.1).

The anteposterior (y-axis) and mediolateral (x-axis) sways are available individually for later analysis. This data is recorded by a force plate, a very sensitive device able to sense a subject's centre of pressure when stood upon. COP trajectories are constantly moving, and it is quantifying the nature of

these movements through modelling which is the topic of this thesis.

1.1 Physiological Background

Identifying the systems involved in quiet stance postural control is important when one wants to develop complex models for the postural control system. There are three sensory input systems within the body that have been identified as contributing information to the postural control system: the Visual, Somatosensory, and Vestibular systems (Shumway-Cook and Woollacott, 2000). Each of these systems collect different sensory information, which are then provided to the central nervous system (CNS) which has to assimilate the information and take appropriate corrective action.

The visual system gives information about the position and motion of the head with respect to one's surroundings. Visual inputs provide excellent references with regards to verticality, as many objects (walls, doors, etc.) are aligned in this direction. Visual inputs are not completely necessary for postural control, as standing with one's eyes closed can be accomplished. These inputs are the easiest to perturb during test procedures, however, which makes them very important. Perturbing an input system is a good way to probe the workings of the control systems using the input. Visual inputs can be perturbed during quiet stance by moving the area around a subject, through the use of a moving room or a moving wall. Removing visual inputs can be accomplished using a blindfold or by asking the subjects to close their eyes.

Somatosensory inputs provide two different types of information to the CNS. One type is in reference to the supporting surface; both position and

motion information with respect to the supporting surface are recorded. The somatosensory system also provides information about the relative positions of various body segments to one another. Receptors for this system are located in the skin, joints, tendons, and muscles. The somatosensory system is the most important system in quiet stance in healthy adults (Shumway-Cook and Woollacott, 2000). The inputs are most useful on a horizontal surface when it is appropriate to be vertical to maintain upright stance. Perturbing the somatosensory system is more difficult than the visual system, as it requires moving the surface on which stance is being maintained. This can be accomplished using special force plates.

The vestibular system provides the CNS with information about the position and movement of the head with respect to inertial and gravitational forces; providing subconscious information only. Inputs are received from semicircular canals, which are most important during rapid head movements, and otoliths, which are most sensitive to slower head movements. The vestibular system on its own cannot maintain upright stance adequately, as it is unable to distinguish between head movements with different causes (i.e., a nod of the head and a slight bow). It is, however, very difficult to perturb the vestibular system, as gravitational forces provide a fixed reference.

The information from each of these three systems is processed by the CNS in the spinal cord and the brain to provide one with postural control. The way the information is combined and utilized is not yet well understood.

Data are collected during quiet stance for several reasons. The relative ease of this activity allows COP trajectories to be collected for most types

of patients. Alternatives to quiet stance include situations such as perturbed stance, where subjects are given a small perturbation during quiet stance. For subjects with very poor balance control, this type of test can pose a danger. There is also some evidence that responses during quiet stance are predictive of those during perturbed stance, which will be discussed in Section 2.3. Other tests can involve an active challenge to balance (such as a moving or compliant platform). Repeated measures with these types of tests can result in subject fatigue and learning, neither of which are of interest in this case. Since it is assumed that accumulated learning and fatigue are minimal for quiet stance, this allows repeated collection on the same patient within a short period of time.

It should be noted that the body, when in quiet standing, is not necessarily attempting to control the COP; rather the body may be more concerned with the position of the Centre of Mass (COM). Movements of the COM are more difficult to measure, and have been shown to correlate very strongly with the motions of the COP. It is COP data, therefore, which are usually used during analyses.

This study deals with comparing the postural motions of Down syndrome (DS) subjects with those of non-DS subjects. Individuals with DS are characterized, in part, by what appear to be "clumsy" movements. Through detailed analysis of COP data, it is hoped to gain insight into possible reasons for this type of movement. Identifying reasons for movement deficiencies can allow for the design of improved treatment regimens in some cases. In particular, those with DS often have low muscle tone, which could lead to movement

problems. Studies such as Latash (2000) have suggested that DS subjects may adopt movement strategies that result in a higher stiffness in the muscles, which can also lead to movement problems. Through the modelling and analysis of COP data, it is hoped to gain insight as to the state of the muscle in a simple, but active, task such as upright stance. In this thesis, two theoretical physical models, the Pinned Polymer and Inverted Pendulum models, are examined which are able to provide what are referred to here as "stiffness measures". The stiffness measure of the pinned polymer model is related to elastic restoring forces, similar to a spring constant. The stiffness measure of the inverted pendulum model relates to the impendence at the ankle joint. These stiffness measures, once estimated from real data, should be related to the true physiological stiffness of the postural system. This relation is only in a general sense, as physiological stiffness itself is not well defined. They are compared here to clinical measures of muscle tone, which do not measure muscle tone during activity.

1.2 Data Collection

Nine adults with DS (3 males and 6 females) and 9 adults without DS (3 males and 6 females) aged between 19-40 years participated in the study (Table 1). Participants were recruited from the university population and through the local Down syndrome support group. All participants gave informed consent for participating in the study, which was approved by the University of Victoria Human Research Ethics Committee. An AMTI AccuSway^{PLUS} Balance Platform was used to collect the COP trajectories. The signals were collected at a frequency of 100 Hz, amplified, filtered (30 Hz) and centered.

Subjects	Age (years)	Weight (kg)	Height (m)
Participants with DS Total n= 9 3 Males, 6 Females	30.8 (6.2) 19-38	69.47 (16.8) 48-96	1.49 (0.1) 1.37-1.68
Participants without DS Total n=9 3 Males, 6 Females	25.1 (5.8) 21-40	65.4 (10.4) 51-86	1.67 (0.12) 1.52-1.93

Table 1. Descriptive statistics of the subject population for age, weight, and height. Values shown are the mean, standard deviation in brackets, and the range (minimum - maximum) of each measure.

As in the general population, those with Down syndrome tend to be shorter; subjects with Down syndrome also tended to be heavier than ones without.

During data collection, a subject first removed his or her shoes and then was told to stand comfortably on the force platform. Foot position was

marked on the platform to ensure consistent foot position and stance width (stance width has been shown to greatly affect the sway of subjects). The subject then stepped off the platform and the force plate was zeroed. The subject then stood back on the force platform with their feet at the indicated positions. Subjects were told to look ahead at a spot on a picture in front of them (positioned on the wall, approximately 2 metres away) and stand comfortably still. Once comfortable stance was achieved (as indicated by the subject), data collection was activated. Each trial lasted for 30 seconds. Once a trial was over, the subject stepped off the platform for a rest period of 20-40 seconds. The platform was re-zeroed during these rests. Once a subject was ready, another trial was collected. Typically twenty trials were collected consecutively by this procedure, a set of ten with eyes open (EO), and a set of ten with eyes closed (EC). The order of the EO and EC sets was randomized. Eyes closed trials were collected in the same manner as eyes open, except subjects closed their eyes and indicated readiness before data collection began. Someone stood near the subjects during EC trial collection; subjects must be watched more carefully as they become more prone to falling. Subjects may also attempt to "cheat" during EC trials by slightly opening their eyes, these trials must be detected, allowing experimenters to collect a replacement trial.

Four basic measures on the COP trajectories, *Velocity, 95% Ellipse Area*, *X-Range*, and *Y-Range*, are directly calculated within the AMTI software and extracted from there. There are many other basic measures calculated by the software, which could be used in analyses of COP data; only the four

measures mentioned are covered in this thesis.

A traditional measure of passive muscle tone was evaluated by a physical therapist on the DS subjects prior to COP data collection using a 5 point scale: low, low-normal, normal, high-normal, or high muscle tone. These measures are compared to the postural stiffness estimates in Section 4.

1.3 Summary of Thesis

This thesis is divided into four main chapters. Chapter 1 provides a brief background on postural control and a summary of the data collection process, with the physical characteristics of the subjects.

Chapter 2 explores the literature which deals with the analysis of COP data, providing background for Descriptive Measures, Stabilogram-Diffusion analysis, the Pinned Polymer model, the Inverted Pendulum model, and the FARIMA model. Results from studies which have utilized these methods are also covered in Chapter 2.

Chapter 3 explores the data analysis procedure for descriptive measures, and the three models listed above. Details are given about the implementation of each model, specifically mentioning software and procedures used. Results from the basic measures and each of the three models are also summarized here in Chapter 3.

Chapter 4 discusses the results presented in Chapter 3 in a clinical light, comparing DS and non-DS subjects. It then proceeds to discuss each of the models in terms of ease of implementation and theoretical validity. Finally,

relationships between the models are explored, and suggestions for how future work on each model might be improved are suggested.

Chapter 5 gives references, and Chapter 6 is an appendix detailing the code used in various software packages for model fitting and data analysis.

Chapter 2

Literature Review

2.1 Descriptive Measures

Much of the previous work done with COP data has involved comparing a subject's balance characteristics under several conditions. The most common test has been to compare an individual's quiet-standing postural sway under eyes open and eyes closed conditions; the Romberg test was developed to accomplish this. The test originally was designed to be used without any instrumentation; clinicians simply compared stability with eyes open and closed. Measures of stability available from COP trajectories have been adapted to this test, including mean square displacement and velocity. These measures are also used individually to compare subjects to one another. Some of these are further described here.

Velocity (or *Total Distance*, velocity multiplied by the total time of the trajectory) is frequently used to compare individuals in different subject

groups. Removing the visual inputs would be expected to increase a subject's instability, as measured here by velocity. For physical reasons, one expects the velocity of the COP to increase for taller subjects as well. Taller subjects are expected to have a faster COP motion and cover a greater area. This can be attributed to the increased height of a subject's COM; a greater height for a balancing point leads to increased velocity and area of sway if angular displacement from the vertical is similar. This may explain why male subjects tend to have greater velocities. Velocity, however, provides little insight as to the cause of postural differences between subjects of similar physical characteristics. This limits the use of velocity, as many different underlying causes could lead to the same observed differences; it can, however, be used to compare severity of problems amongst subjects known to have the same physical/mental conditions.

Sway Area can be measured in many different ways. One method is to choose the smallest shape (circles, rectangles, and polygons are all used) that encompasses all of the data. Another method uses the assumption that the anteposterior (A/P) and mediolateral (M/L) data are distributed under a bivariate normal distribution. Under this assumption, an ellipse can be calculated based on the means, variances, and covariances of the two components of the COP trajectory that should cover 95% of the data. The assumption of bivariate normality is not always justified by the nature of the data, but as many COP trajectories have a small amount of data that is greatly different from the rest (see Figure 2.1), this allows a summary measure of area that is relatively unaffected by small excursions from the

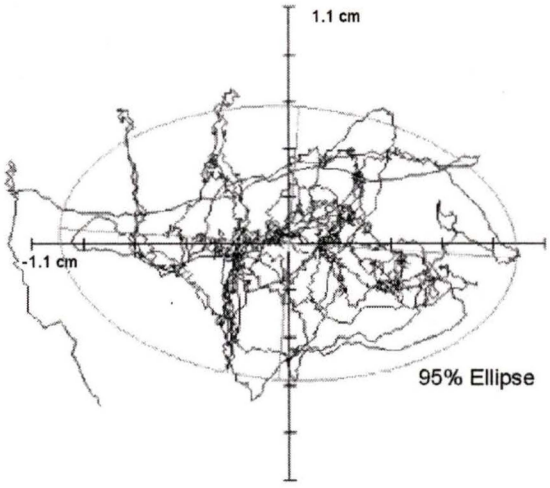

Figure 2.1: A COP trajectory showing an excursion from the bulk of the data. The 95% Ellipse is also shown.

bulk of the data. 95% sway area is therefore only an approximate measure, not necessarily covering 95% of the data. As with velocity, sway area provides no insight as to the cause of these differences.

X-Range and *Y-Range*, which record the maximum difference in displacement from centre in the mediolateral and anteposterior direction respectively, are also explored here. The main usefulness of both of these measures is to quantify the entire range of movement. As opposed to sway area, x-range and y-range do not attempt to ignore the occasional excursions from the bulk of the data. These are reported here mainly as they are commonly reported in the literature in studies using a force platform.

In all of the descriptive measures calculated from a COP trajectory, no

attempts are being made to compensate for the natural differences between subjects, such as height (as discussed earlier), or weight. If measures such as velocity were used to make diagnoses, differences such as these may be confused with the presence of an actual disorder. It is for reasons such as this that further research is being done using COP data more intelligently; not just the amount of movement of the COP is being investigated, but the characteristics of these movements as well. The characteristics of COP movements (measures such as correlation and autocorrelation) are the primary concern of this thesis. An important first step is the identification of COP movements as a randomly driven process (Collins and De Luca, 1994).

The irregular output of postural control systems, as demonstrated by the appearance of a COP trajectory, makes it a possible candidate for physiological chaos. Physiological chaos has been suggested as the underlying driving force in the nervous and muscular systems at rest in mammals. If postural control systems also behaved in this way, it may suggest new treatments for instabilities. Algorithms able to detect the presence of an attractor and sensitive dependence on initial conditions (both characteristics of chaotic systems) have been developed recently and applied by Collins and De Luca (1994) to COP data. Their conclusions were that COP trajectories are not an instance of chaos, and were instead better described stochastically. Collins and De Luca (1993) had previously modelled COP data as a random walk process, using a technique they developed called stabilogram-diffusion plots.

Basic measures on COP data have been used in many previous studies to help differentiate various pathologies from normal subjects. Conditions in-

clude Down syndrome (Vieregge et al., 1996), Parkinson's Disease (Viitasalo et al., 2002), advanced age (Melzer et al. 2000), Friedreich's ataxia as well as several types of brain lesions (Diener et al., 1984), spasticity (Nardone et al., 2001), and hemiplegia (Shumway-Cook et al., 1988). Other studies have looked at changing the conditions of balance for a normal subject population through cognitive and physical tasks (Maylor and Wing, 1996; Hunter and Hoffman, 2000), with similar goals in mind. In all of these studies, various measures taken from COP trajectories, such as velocity, sway area, sway path, sway range, and others, are used to attempt to differentiate the subjects with a condition of interest from either normal subjects (as is usually done), or from other stance conditions.

Subjects with Down syndrome were found to have, as compared to similarly aged controls (age range 19-42 for Down syndrome, 23-37 for non-DS), significantly higher velocities under both EO and EC conditions, as well as higher Sway Area (similar to 95% ellipse area) and A/P Sway (similar to y-range) under EO conditions (Vieregge et al., 1996).

Subjects with Parkinson's disease in the the age range of 50 to 83 as compared to control subjects from age 46-77 showed significantly higher velocities and areas under both EO and EC conditions (Viitasalo et al., 2002). X-range was also significantly higher under both visual conditions. Further comparisons within the PD group showed significant differences in velocity, area, and x-range. These differences showed those that patients who had PD for a longer time had higher values for those measures.

Studies on those with advanced age, defined as ages 75-84 in Melzer et al.

(2001), have revealed that as compared to young subjects (ages 20-34), they have significantly greater postural characteristics in each of the measures velocity, elliptical area, x-range, and y-range. These differences are present in two different stance widths under EO conditions.

The study by Diener et al. (1984) compared data from six groups of subjects: controls (no disorders present), those with Friedreich's disease, and those with four other conditions affecting the cerebellum. The study used many different measures taken from EO and EC COP data collections, including sway area, velocity, A/P and M/L range, and the Romberg quotient. The Romberg quotient is defined as the ratio of velocities between EC and EO conditions. A Romberg quotient of over 1 indicates an observed increase in velocity under the EC condition. "Pathological results" were defined as exceeding the over-all-group mean by more than 2 standard deviations (Diener et al., 1984); the percentage of each patient group falling in each of these groups were recorded. Using velocity, sway area, and A/P sway the various groups gave pathological results 77-86% of the time. Analysis of variance and subsequent multiple comparisons were carried out to distinguish between patient groups. These analyses primarily distinguished between controls and those suffering, "*...from a late cortical atrophy of the anterior lobe...*" (Diener et al., 1984). Patients with legions of the cerebral hemispheres were not significantly distinguished by the use of the available COP measures, although other observations did show promise in locating (distinguishing) existing cerebral lesions.

These results only reveal existing differences, providing little insight as

to the root causes of postural sway characteristic differences. Through modelling of the postural system it is hoped that differences in postural sway characteristics will be shown, but more importantly it is hoped to discover some of the postural system differences which underly these differences.

2.2 Stabilogram-Diffusion Analysis

The idea of the stabilogram-diffusion (S-D) analysis developed by Collins and De Luca is that a COP trajectory, "*can be modelled as a system of coupled, correlated random walks, i.e., the motion is considered to be the result of a combination of deterministic and stochastic mechanisms*" (Collins and De Luca, 1993). One-dimensional Brownian motion (the random movement of a particle along a straight line) is used in the modelling procedure. The mean square displacement is defined here as:

$$\overline{\Delta x^2}_{\Delta t} = \frac{\sum_{i=1}^{N-m} (\Delta x_i)^2}{(N-m)} \tag{2.1}$$

where $\Delta x_i = x_i - x_{i+\Delta t}$, x_i refers to the mediolateral displacement of the COP at time point i, N is the total number of data points, and m is the number of data points in the time interval Δt. m points are omitted from the summation as m many data points do not have a corresponding time point Δt later, i.e., a point closer than m time points from the end of the trajectory cannot be used in the calculation. Similar formulae to 2.1 hold for the anteposterior direction, referred to as y, and the two-dimensional

trajectory (x,y), referred to as r. As $\overline{\Delta r^2}$ is equivalent to $\overline{\Delta x^2} + \overline{\Delta y^2}$, it need not be calculated separately. The measure $\overline{\Delta x^2}$ was shown in 1905 by Einstein, under the assumption of Brownian motion, to be related to Δt by:

$$E[\Delta x^2{}_{\Delta t}] = \overline{\Delta x^2}_{\Delta t} = 2D\Delta t \tag{2.2}$$

where D is the diffusion coefficient, which is a measure of the activity within the random walk. Brownian motion is characterized by two properties. These properties are

$$E[\Delta x_{\Delta t}] = 0, Var\,(\Delta x_{\Delta t}) = \sigma^2 \Delta t. \tag{2.3}$$

From (2.3), one can see that D from (2.2) also provides an estimate of the variance of the increments, as $D = \sigma^2/2$. Equation (2.2) applies to x, y and r here, and is fit for all three by Collins and De Luca (1993). Brownian motion has been generalized to fractional Brownian motion (Mandelbrot and van Ness, 1968), which was introduced to describe Gaussian stochastic processes. Fractional Brownian motion is indexed by the Hurst parameter $H \in$ (0,1). Such processes, in finite dimensional space, were introduced originally by Kolmogorov in 1940, with Mandelbrot and van Ness providing some properties in later work. For the model here, the most important result is that (2.2) generalizes to:

$$\overline{\Delta x^2}_{\Delta t} = 2D\,\Delta t^{2H} \tag{2.4}$$

H here is the scaling exponent, and can take on values from 0 to 1. D can be estimated directly from the slope of $\overline{\Delta x^2}$ versus Δt, and H can be estimated

from the slope of $\overline{\Delta x^2}$ against Δt on a log-log scale. An H of 0.5 corresponds to classical, or completely random and uncorrelated, Brownian motion. For H, a value less than 0.5 means that the random walk is negatively correlated. A negatively correlated random walk is anti-persistent, meaning trends in the motion tend to reverse themselves more often than in classical Brownian motion. For H greater than 0.5, the random walk is persistent and thus tends to continue previous trends in the motion.

Stabilogram-diffusion plots, which are plots of mean square displacement against the time interval (as in Figure 2.2), reveal two regions of differing slopes. The presence of these two different regions, one for very short term intervals (on the order of 1 second), and another for the intermediate time intervals, has been interpreted as the body shifting from open-loop to closed-loop control mechanisms (Collins and De Luca, 1993). An open-loop control mechanism is characterized by persistence, or the tendency of that being controlled to continue in its current direction. Closed-loop control mechanisms demonstrate anti-persistence, or a tendency to correct against the current movements. A third region of zero slope is also expected to occur for very long intervals. Maintaining postural control bounds the range of the COP; reaching the outer bounds causes the breakdown of the correlation structure. Thirty second trials, however, may not be long enough for this third region to appear reliably, as it is only expected in long-term behaviour. Open-loop control mechanisms are expected under the hypothesis that postural control systems allow small movements of the COP. These are allowed to go uncorrected as they do not put individuals in an off-balance position. After a

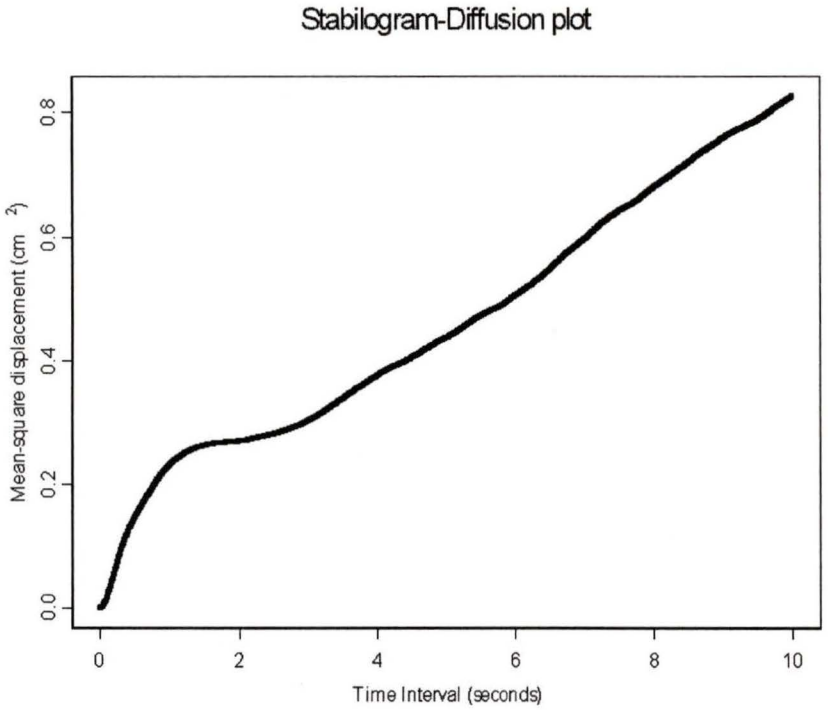

Figure 2.2: A stabilogram-diffusion plot as described by Collins and De Luca (1993).

certain amount of time and/or displacement from relative equilibrium, however, closed-loop control systems will attempt to return the body to a relative equilibrium. This type of control system is expected to be observed in each of the x, y, and r trajectories. The analysis therefore provides twelve parameter estimates: D_{xs}, D_{xl}, D_{ys}, D_{yl}, D_{rs}, D_{rl}, H_{xs}, H_{xl}, H_{ys}, H_{yl}, H_{rs}, and H_{rl} (the subscripts s and l here refer to short-term and long-term respectively).

Results given by Collins and De Luca (1993) show that D and H can be repeatedly measured on a subject with some consistency. Intraclass cor-

relation coefficients (ICCs) were calculated for the D and H values for the x, y, r in each of the two regions. Thirty trials were conducted on each of ten subjects and were split into three groups of ten trials. S-D plots were calculated for each individual trial, and these were averaged within the group of ten trials to produce three plots for each subject. This provided repeated measures on each subject. The values of the ICCs indicated good to excellent reliability for most of the D and H parameters. The D and H values can be interpreted as relating to the stochastic activity of an individual and the regulation of the postural control systems. These interpretations, however, do not provide a great deal more information than previous measures such as velocity or sway area. The location of the transition point between the two slope regions was the least consistent measure of those collected. This point is interpreted as the transition from the open-loop to the closed-loop control system. It is not explained why the estimates of this point are so variable, and many possible explanations are given that may explain the existence of this transition point.

Collins and De Luca (1994) also showed that COP trajectories are consistent with the hypothesis that they result from a system based on correlated noise. This is as opposed to resulting from a chaotic system. Testing was done by creating surrogate data sets based on the original COP trajectories. A Fourier transform was taken, the phase information randomized, and an inverse Fourier transform was done. Test results did not significantly differ between the original and surrogate data sets, indicating that the null hypothesis, of a correlated noise system, not be rejected.

In one of the first applications of the S-D analysis (Collins and De Luca, 1995), an unexpected result was obtained; it was shown that among 25 healthy subjects, 13 had a greater D_{rl} (two dimensional long-term diffusion coefficient) under eyes-closed conditions (as compared to eyes-open conditions), while 12 had a smaller D_{rl}. Many previous studies have shown that sway increases for almost all subjects under eyes-closed conditions. The two groups of subjects had no significant differences in measured characteristics (age, weight, height), so the authors split the subjects into two groups based on the newly discovered dichotomy. Within these two groups there are significant differences in the nature of the changes of some D and H parameters between eyes-open and eyes-closed trials. Interestingly, the group of twelve subjects showed no significant differences between eyes-open and eyes-closed in more traditional measures (velocity, radial area), whereas the group of thirteen subjects did (Collins and De Luca, 1995). These facts lead the authors to hypothesize that visual input is affecting the activities of postural control systems differently in the two groups. Further discussions of the two groups and possible explanations for the findings can be found in Collins and De Luca (1995). The critical points between regions were further explored in this paper as well. Occurring at approximately 1 second in both groups and under both eyes-open and eyes-closed visual conditions, several possible explanations for its existence (Collins and De Luca, 1993) are rejected. Preprogrammed commands in the postural control system are given as the most likely explanation given the findings of their study.

The S-D analysis revealed several important features of COP trajectory

data, especially in regards to the correlation structure. The analysis produces significant results when comparing eyes-open and eyes-closed conditions, and may have identified the existence of two different postural control strategies in use by the general population. The diffusion coefficients and scaling exponents, however, do not have direct physiological interpretations such as, "*high D_{rl} values indicate a high muscle stiffness*". This limits the effectiveness of the analysis, which likely explains why one of the main authors, Collins, moved on to a more physiological model of postural control, the pinned-polymer model.

2.3 The Pinned Polymer Model

The Pinned Polymer model was introduced by Chow and Collins (1995) as an extension of the S-D analysis. The main observation of the S-D method was the presence of the three regions of different scaling. In terms of H, these regions had $H \approx \frac{4}{5}$, $H \approx \frac{1}{4}$, and $H \approx 0$. These regions were noted to be similar to, "*...the behaviour of the dynamic fluctuations of surface or interface growth, flux lines in super-conductors, and polymers*" (Chow and Collins, 1995). The first scaling region, which in postural control corresponds to short-term inertial effects, is often not considered important in other physical processes. Chow and Collins (1995) assume that the short-term effects are important in postural control, and in fact give clues as to the type of control system which is in place for the postural system. The second scaling region is present in theories of the above processes, "*...where nonlinearities do not play a role*"(p 52). The presence of a third scaling region indicates the system has a time scale where all long-term correlations are cut off. In polymer models, this occurs in dynamic fluctuations of a polymer when it is pinned in space to a fixed region (Chow and Collins, 1995). It is this observation which later leads to the "pinning" of the model to a fixed point.

The goal of the pinned polymer model is to model the anteposterior (y) movements as a function of time t and height z, i.e., y can be thought of as $y(z,t)$. A single dimension is analysed here because it was found (Chow et al., 1999) that the movements of the COP correlate to a very high degree, 0.94 $\pm$ 0.02, with the movements of a single marker in the hip. The movements

of the hip likewise strongly correlate with movements of the center of mass (COM), typically located near the middle of the hips. It is the position of the COM which is controlled by the postural system, but it is difficult to measure directly.

Modelling the body as a flexible rod, or polymer, under tension with friction yields the standard equation (Chow and Collins, 1995) describing the forces of the system:

$$\rho\,\partial_t^2\,y + \mu\,\partial_t\,y = T\,\partial_z^2\,y \tag{2.5}$$

where ρ is mass density (kg), μ is a friction coefficient with units kg/s, and T is the tension, with units of $kg \times m^2/s^2$. Under this model, the polymer has an inverted pendulum instability. Due to the challenges of upright stance described in earlier sections, this control system is very complicated and necessarily imperfect. This places upright stance under constant stochastic fluctuations. The system as described by (2.5) does not include attachment to the floor, as one has during quiet stance at the feet. The system is simpler analytically when the polymer is assumed to be of infinite length. Note that in the end the modelling will only be done on one point on the polymer. Adding this assumption to the pinning force and the stochastic fluctuations, the pinned polymer model becomes, as represented in Figure 2.3,

$$\rho\,\partial_t^2\,y + \mu\,\partial_t\,y = T\,\partial_z^2\,y - Ky + F(z,t) \tag{2.6}$$

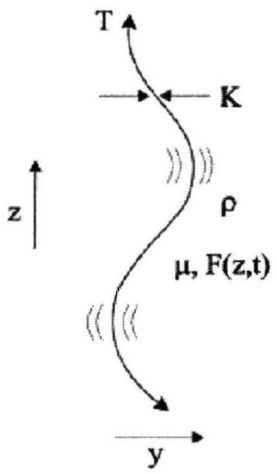

Figure 2.3: The Pinned Polymer model is represented here, with the forces in (2.6) shown.

where K is the elastic (pinning) constant (kg/s^2), and F the stochastic force, in units of N. Dividing (2.6) through by μ and relabelling gives:

$$\beta\,\partial_t^2 y + \partial_t y = \nu\,\partial_z^2 y - \alpha y + \eta(z,t) \tag{2.7}$$

Written as such, β and α^{-1} have units of time, while ν is in length squared divided by time. Parameters β and α, as well those contained in the stochastic force η, are free in this system. The deterministic parts of (2.7) describe a polymer under tension embedded in an elastic membrane, with friction. The parameters of the model also have physical interpretations at this point. ν represents the stiffness (tension) of the system, but is difficult to measure directly. Dimensional analysis leads to the conclusion that $\nu \sim (\alpha/\beta)L^2$ (Chow

et al., 1999), where L is the length of the original rod described by (2.5). As it is proportional to the tension in the system, the quantity $K = \alpha/\beta$ is defined as the normalized stiffness of the system (Chow et al., 1999).

Detailed Fourier analysis of the differential equation (2.7) (Chow and Collins, 1995; Chow et al., 1999; Lauk et al., 1998) has yielded the result that the system can be described by a Bessel function. This was found through the relationship, in (2.7), between the response function and the derivative of the autocorrelation function. Defining a response function as a functional description of a system's response to perturbation over time, "the analytically calculated response function $R(t)$ for the pinned polymer model is given by

$$R(t) = \Theta(t)\frac{e^{-t/2\beta}}{2\sqrt{\upsilon\beta}} J_0\left(\frac{\sqrt{4\alpha\beta - 1}}{2\beta}t\right) \tag{2.8}$$

where J_0 is the zeroth-order Bessel function and Θ is the Heaviside step function (Chow and Collins, 1995). In instances where $4\alpha\beta<1$, the argument of the Bessel function is a complex number. This gives the result

$$R(t) = \Theta(t)\frac{e^{-t/2\beta}}{2\sqrt{\upsilon\beta}} I_0\left(\frac{\sqrt{4\alpha\beta - 1}}{2\beta}t\right) \tag{2.9}$$

where I_0 is the zeroth-order modified Bessel function. Bessel functions can be easily approximated, so now it is possible to fit the model to a proper transformation of the data, i.e., the derivative of the autocorrelation function of a COP trajectory. It has been shown (Chow et al., 1999; Lauk et al., 1998) that, in the case of the PP model, $R(t)$ is directly proportional to the

derivative of the autocorrelation function of the A/P component of a COP trajectory,

$$R(t) \sim \frac{dC(t)}{dt}. \tag{2.10}$$

where $C(t)$ is the autocorrelation function. Once the derivative of the autocorrelation function has been properly normalized, it can be fit to Bessel function models as well, as in (2.8) and (2.9).

Once the model had been established theoretically, Lauk et al. (1998) performed a model check as follows. As the model predicts that the nature of the movement in response to perturbation and quiet stance should be proportional, experiments were done to check this. These experiments involved ten young healthy adults, for each of whom 10 quiet stance trials of 90 seconds and 20 perturbed stance trials of 60 seconds were collected. The perturbed trials were done by applying a weak mechanical force ($\sim$7.35 N) on the subject's pelvis. Reasons were not stated for why they ran 20 perturbed trials versus 10 unperturbed trials. The experimenters may have been worried about falls during trials, which would not provide the desired information. This force was applied randomly 15 to 20 seconds into the trial to avoid the subject adjusting for the force before it was applied and to allow for quiet stance to be achieved before and after the perturbation. Two estimated quantities, $R(t)$ and $dC(t)/dt$ were calculated from these trials. $R(t)$ is the average of the perturbed trials, where averaging begins at the maximal amplitude in sway achieved after perturbation. $dC(t)/dt$ was estimated by

averaging the negative derivatives of the autocorrelation functions of the unperturbed single trials. Each negative derivative was averaged starting from the maximum value the negative derivative achieved, as in Figure 2.4. This was done after normalization by the value of the maximum point, so that each trial began at a value of 1 for the first averaged point. Errors at each time point in each quantity were taken to be the standard deviations of the average at each time point.

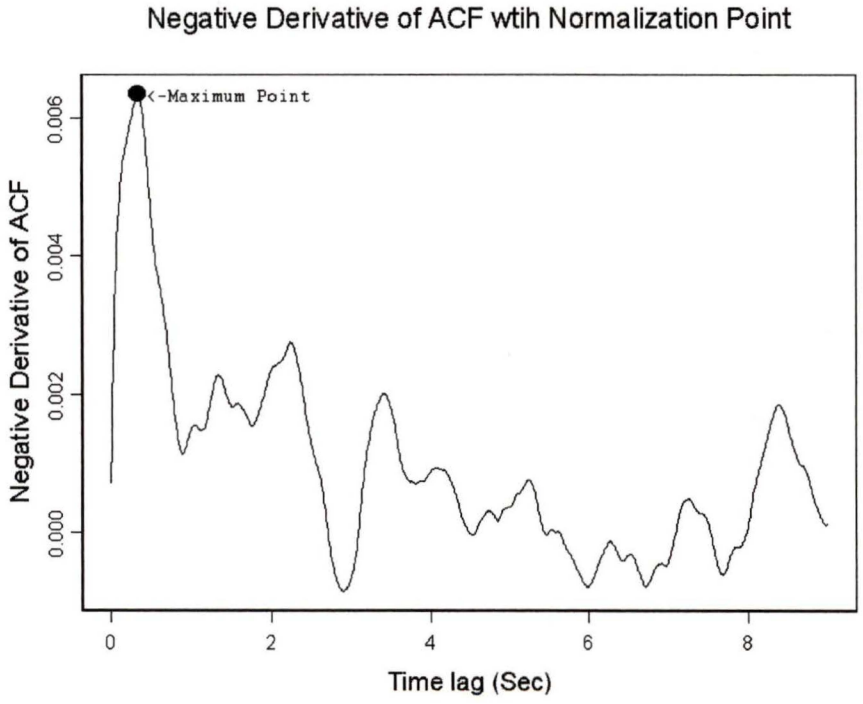

Figure 2.4: Shown is the negative derivative of the ACF, as well as the maximum point, whose location and value are used for normalization

To assess the pinned polymer model, a linear regression model was fit using $R(t)$ as the dependent variable and $dC(t)/dt$ as the explanatory variable. $dC(t)/dt$ was estimated using the first differences of the autocorrelation function (Lauk et al., 1998). The goodness of these fits on each subject was judged by an estimated χ^2, which is the sum of squared residuals weighted by the errors in each original measure. The fit was done for the first 4 seconds of the trials, providing 400 data points (data was collected at 100 Hz). The results from this procedure were mixed; seven of the ten subjects had a good fit as defined in Lauk et al. (1998) as having an estimate of χ^2 between 300 and 480, while three did not have a good fit (χ^2 over 800). While this provides good evidence that a relationship is often found as expected, the small number of subjects here makes it difficult to assess the reliability of predicting $R(t)$ from $dC(t)/dt$. Some possible explanations are provided as to why the regression did not provide a good fit in three cases. It was theorized that subjects may have adopted abnormal strategies to compensate for the unusual situation.

Further assessment of the pinned polymer model was done by fitting the Bessel function model directly to $R(t)$ and $dC(t)/dt$. This was done using the Levenburg-Marquardt (L-M) method. Details of this type of fit are provided in the next chapter. The model predicts that $R(t)$ and $dC(t)/dt$ should both take the form of a Bessel function as defined in (2.8) and (2.9). Assumptions were made that the estimated standard deviations (from trial averaging) were normally distributed, although this assumption was not checked. The advantage of this assumption is that the standard errors for the parameter

estimates can be extracted from covariance matrices used in the L-M method. Using a χ^2 goodness of fit criterion, data from nine of ten subjects gave a good fit to the predicted model given by (2.8) and (2.9) (the one subject who did not provide a good fit was not described) for both $R(t)$ and $dC(t)/dt$. This shows that postural control, at least over short time intervals, seems to obey the fluctuation dissipation theorem (FDT) fairly well. After the passage of too long a time period, non-stationary effects may enter into the data. As subjects adjust their balance the point upon which balance is being maintained may shift. The model is unable to compensate for such effects.

As $R(t)$ and $dC(t)/dt$ behave in similar manners, and one is usually predictive of the other, it can be inferred that postural control systems do not react differently to external perturbations than those caused by internal fluctuations. That is, if the postural control system is brought to a non-equilibrium state, it does not matter how it arrived at that state. This allows the study of postural control to be done under quiet stance conditions, with the results also being applicable to perturbed stance. As many patients for whom balance control is an issue would be unable to perform perturbed trials without risk of injury, this is an important result.

This model was applied to a group of eighteen Parkinson's Disease patients in a separate study by Lauk et al. (1999). The purpose of the study was to see if results obtained from the pinned polymer model agreed with pre-existing clinical measures of the severity of Parkinson's Disease (PD). The parameter of interest from the pinned polymer model was the normalized stiffness $K=\alpha/\beta$.

Ten 30 second trials were collected on each subject under eyes open, unperturbed stance conditions. For each of the collected trials, the autocorrelation function was computed. The negative slope of the autocorrelation was estimated via a simple two-point filter. The resulting series were then normalized. This was done using the time of maximum amplitude as the key point; the series were cut-off at this point, and each was normalized by the value at the maximum amplitude. This results in ten series per subject which all begin at exactly 1 and are unit-free. These ten trials were averaged, with this trial average being fit to

$$e^{-t/2\beta} J_o \left(\frac{\sqrt{4\alpha\beta - 1}}{2\beta} t \right) \tag{2.11}$$

using the L-M method (sample point-wise standard deviations also are used in the L-M method). (2.11) is the simplified version of previous PP model representations, with ν removed from the equation. The estimates and standard errors of α and β were used to give the estimate of K. The reliability of K was also checked in this study by breaking the ten trials for each subject into two random groups of five trials and performing the analysis on these groups. The Pearson correlation coefficient between the two K estimates across the eighteen subjects was as high as 0.9 (random groups of five trials were apparently selected several times to be sure of consistent results). This indicated that K was very reliable.

Comparisons in Lauk et al. (1999) were based on Kendall's rank correlation coefficient (Kendall's τ), a non-parametric statistic. A large value for Kendall's τ indicates a rank correlation between K and a clinical mea-

sure (low clinical measure tends to give a low K, high measure gives high K). The results of these comparisons were that K correlated significantly with the clinical measures of Rigidity, Bradykenesia, Posture and Leg-agility, Retropulsion test score, and Gait, the first four of which are measured in the same standard clinical test (UPDRS). Three measures did not give significant correlations, resting-tremor severity, postural-tremor severity, and the UPDRS component that gives a measure of a subject's ability to rise from a chair. Tremor measures have previously been shown not to correlate with falling in PD patients. The results here show that the stiffness measure K, which is obtained objectively and noninvasively, may be very useful to obtain on a patient. Also, traditional measures (Sway area, Velocity) on quiet stance COP data from PD patients are not able to distinguish them from the healthy population, so it provides a validation of the use of more complicated analyses on the COP trajectories.

The Pinned Polymer model shows a great deal of promise in modeling the dynamics of postural control. There are several assumptions made in the course of the analysis, however, that call it into question. A basic assumption made when measuring body sway is that the postural control systems are interested in regulating the COM. The COP is used as an estimator of the COM, and it does correlate very strongly with it. The models discussed in the next section deal with the nature of the difference between the COP and the COM. The model assumes that the system is always attempting to return to the same relative equilibrium (i.e., postural control systems are stationary). This assumption is acknowledged as not being accurate, as the

postural systems change within a given data collection. The importance of this assumption is lessened by examining the autocorrelation over only a short time period (4-6 seconds), but not totally overcome. The analyses done in the final section of this chapter attempt to deal with this non-stationarity.

2.4 The Inverted Pendulum Model

The idea behind the stiffness control model, as proposed by Winter et al. (1998), is that upright stance could be maintained in the body through regulation of muscle stiffness alone. The basis of the model is that the body acts as an inverted pendulum during upright stance. The proposed model assumes that, "*... muscles act as springs to cause the center-of-pressure (COP) to move in phase with the center-of-mass(COM) as the body sways about some desired position*". An important difference between this model and previous ones is that the COP position is no longer used to directly estimate the COM position for balance control (as done in Stabilogram-diffusion analysis and the Pinned polymer model). Instead, both the COP and COM are directly measured, and the difference between these measures is analysed. Several conclusions are reached by Winter et al. (1998) that were later disputed by Morasso and Schieppati (1999) on the basis of further analysis of the natural dynamics of the model.

The inverted pendulum (IP) model gives a relationship between the COM and the COP, which are respectively treated as the controlled and controlling variables of the system. This means that in order to control the position of the COM, and hence balance, the body can control the COP position. In the anterior-posterior plane, the relationship can be derived from the model. Defining, as shown on Figure 2.5, h as the height between the ankle joint and the COM, y as the location of the COM (as defined by the displacement from the ankle joint), R_v as the vertical ground reaction force located p_y from

the ankle joint. p_y is the location of the COP. Further, R_y is the horizontal ground reaction force, oriented in the same direction as the current COP movement. Both y (the COM) and p_y (the COP) can be thought of as functions of time, as they are measured over the course of data collection. W is defined as the body weight above the ankle joint, which is equal to the vertical reaction force R at the ankle. Where m_f is the mass of the feet and g is the gravitational constant, in quiet stance conditions, the vertical forces balance through the following equation:

$$R_v = -R + m_f g. \tag{2.12}$$

This equation simply states that forces of the system acting downwards, $-R + m_f g$, must be equivalent to those acting upward. In this system, the vertical ground reaction force R_v accounts for virtually all of the force acting upwards. In quiet stance, horizontal ground reaction force is quite small and can be ignored. The moments acting around the ankle joint can be written as

$$M_a + R_v p_y - m_f g y_a = t I_f \alpha_f \tag{2.13}$$

where α_f is the angular acceleration of the foot, I_f is the inertial moment of the foot, y_a is the horizontal distance from the centre of mass of the foot to the ankle joint, and M_a is the moment about the ankle joint. α_f is 0 in

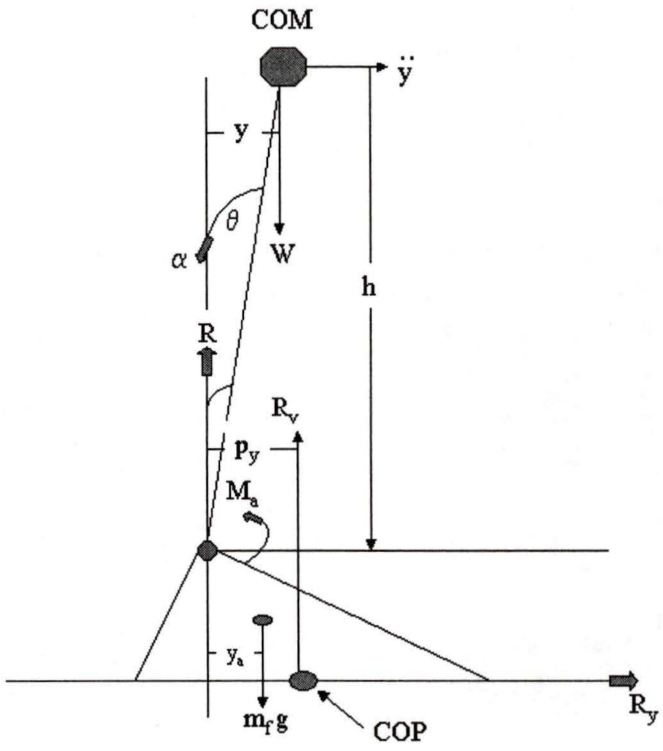

Figure 2.5: Diagram shows the forces acting on the postural system in the inverted pendulum model (Winter et al., 1998).

quiet stance as no foot displacements are occurring, and $m_f g(y_a - p_y) << Rp_y$. This inequality follows from physical properties of the system. The mass of the foot m_f and the distance between the COM of the foot and COP $(y_a - p_y)$ are both relatively small. This leads to the conclusion that

$$M_a \approx Rp_y \tag{2.14}$$

Considering the free body diagram of the inverted pendulum acting at the ankle joints tells us that

$$M_a - Wy = Rp_y - Wy = I_{sa}\alpha \tag{2.15}$$

where I_{sa} is the moment of inertia of the body above the ankle about the ankle joint and α is the angular acceleration. As quiet stance produces only small α, meaning that $\tan\alpha \approx \alpha$, it can be approximated by $\alpha \approx -\ddot{y}/h$. $\ddot{y}$ is the acceleration of the displacement from the ankle joint. Vertical reaction force is equal to the weight being applied to the ankle joint (i.e. $W = R$). These give us a relation between the locations of the COP and COM as

$$p_y - y = -\frac{I_{sa}}{Wh}\ddot{y}. \tag{2.16}$$

This tells us that the COM-COP $(y - p_y)$ position difference is proportional to the acceleration of the COM movements. The proportionality depends on the weight and height of the individual (previous models did not account for body shape). Further, (2.16) tells us that the movement of the COP (p_y) and the acceleration of the COM $(\ddot{y})$ should be out of phase with one another.

Analysis of this model under the assumption of spring-like muscle behaviour is also revealing. As stated in Winter et al. (1998), "*the moment due to the spring, $K\theta$, balances the moment about the ankle joint, $Wh\sin\theta \approx Wh\theta$, where K is the rotational spring stiffness...*"(Winter et al, 1998).

Balancing the energy equation for the system, this gives, in units of Joules,

$$K\theta - Wh\theta = -I_{sa}\ddot{\theta}. \tag{2.17}$$

For small angles of sway (θ is the angle of the pendulum from vertical), $\theta \approx \quad y/h$. Using this with (2.17) gives

$$\frac{Ky}{Wh} - y = -\frac{I_{sa}}{Wh}\ddot{y} \tag{2.18}$$

which is identical to (2.16) except for the first term. Ky/Wh must therefore be equal to p_y. This tells us that p_y must be proportional and in phase with y. If the stiffness K is greater than Wh, the system will naturally oscillate and p_y will be larger than y, in the sense that it will oscillate to greater extremes.

The natural, undamped frequency of oscillation of this system

$$\omega_n = \sqrt{K_e/I_{sa}} \tag{2.19}$$

is a function of the stiffness and inertia, with units of rad/s. $K_e = K - Wh$ is the effective stiffness of the inverted pendulum (gravity acts to reduce stiffness through the "gravitational spring" Wh). The simplified stiffness model will oscillate at this natural frequency; it is observed, however, that neither the COP or COM oscillate at a single frequency. This indicates energy is continually entering the system; as a result, the system forms a tuned mechanical circuit. As the stiffness of the system, K_e, is what is of interest here, it is that which is to be estimated. Noting that the stiffness of the system de-

termines the acceleration of the COM, and that (from (2.16)) the COP-COM difference is proportional to this, K_e can be estimated by an analysis of the amplitude spectrum of the COP-COM difference. The amplitude spectrum is estimated by a fast Fourier transform and then converted to a log scale. The resulting equation is described by

$$A(\omega) = \frac{C}{\sqrt{1 + \left[\frac{I\omega}{B} - \frac{K_e}{\omega B}\right]^2}} \tag{2.20}$$

where I and B are the inertial and damping constants and C is a constant. I is determined by anthropometric measures, to be described in the next chapter. This equation can be fit to data using non-linear methods, with B, C, and K_e as the unknown parameters. This allows ω_n to be determined from (2.19); the frequency (in Hz) corresponding to the ω_n is $f_n = \omega_n/2\pi$.

In order to test the validity of the model, Winter et al. (1998) use the relationship between the magnitude of COM sway and K_e, but under a simplified version of the model with no damping of the oscillations. The magnitude of sway, $y(t)$ is

$$y(t) = \sqrt{\frac{y_o^2\omega_n^2 + V_0^2}{\omega_n^2}} \sin(\omega t + \phi) \tag{2.21}$$

where V_0 is the velocity of the COM (in the anteposterior direction) while at zero displacement, ϕ is the angle between a horizontal line at the ankle joint and another line connecting the ankle joint to the COM, and y_0 is the displacement of the COM at $t = 0$. If the model begins oscillating at $y_0 = 0$

at $t = 0$ and $\phi = 90^0$, the magnitude of sway, Y, is given by (utilizing (2.19))

$$Y = \frac{V_0\sqrt{I_{sa}}}{\sqrt{K_e}} \tag{2.22}$$

This means that the displacement of the COM should be proportional to $K_e^{-0.5}$. Checking the observed relationship provides a check of the model. Equation (2.19) cannot be used to directly find K_e as the model of interest has a damping component, and V_0 is unknown as the position of zero displacement is also unknown.

Winter et al. collected data on ten young adults with no known balance pathologies. Subjects stood at three different stance widths, 50%, 100%, and 150% of the hip joint distance, for two minutes each on two force platforms, one for each foot. Eyes closed trials were also performed at 100% stance width. The COM was estimated using OPTOTRAK, a system that tracked the movement of each of 21 markers placed on each subject. These markers were tracked in three dimensions at a frequency of 20 Hz. The COM was calculated as a weighted average of the various segments of the body (limbs, torso, head, etc....) as detailed in Winter (1990). This provides an estimate of the COM every 50 ms. The estimate of the COM may be biased, as the calculations are based on an "average" distribution of mass in each of the body segments. Due to the small movements of the COM during quiet stance, this bias should remain relatively constant over the 120s. Using (2.16), this bias is removed by making the average COM position equal to the average COP position over each trial. The COP was calculated from the data recorded on

the separate platforms and is considered extremely accurate. The validity of using (2.16) in this way is demonstrated by the appearance of the COP-COM difference after the bias removal; the COP oscillates on either side of the COM for the entire 120s.

Once the data has been collected, a curve is fit to the power spectrum of the COP-COM difference via (2.20), yielding f_n (frequency) and B(damping coefficient). Through f_n, ω_n and K_e can be calculated. Many different data analyses were pursued, which are summarized as follows. To check the validity of (2.16), correlations were calculated to compare the COP-COM difference and the COM acceleration, both of which are measured directly (note that the bias removal should have no effect on the correlations). A perfect fit to the proposed model would yield correlations of –1(completely out of phase); for the three EO stance widths, the correlations were (average $\pm$ SD): –0.902 ($\pm$ 0.048), -0.914 ($\pm$ 0.039), and –0.898 ($\pm$0.055). These results were seen as a strong validation of the proposed model. COM displacement was shown to be proportional to $K_e^{-0.55}$ in the mediolateral (M/L) direction via a power curve fit of COM sway versus K_e (analogous results were not given for the anteposterior direction). The COP was found to be slightly larger than the COM at the extremes, as the model predicts. Time shift was calculated between the COM and COP by finding the peak of their cross-correlation. In the anteposterior direction, no significant differences were found for any of the measures (COM absolute sway, COP absolute sway, COP-COM absolute difference, f_n, K_e, B and time shift) over the three EO stances. This was not unexpected, as the base of support for the A/P di-

rection does not change over the stances. In the M/L direction, COM and COP sways became significantly smaller as stance became wider. f_n and K_e significantly increased with stance width, B showed a significant increase only between the last two stance widths. Over all EO stances and directions, the time shift was between –6.0ms (±14.3) and 0.0ms (±4.7), indicating that the COP and COM are in phase.

The results outlined here, as well as other results not reviewed, provide Winter et al. (1998) with justification of their model. The inverted pendulum model as described has muscle stiffness in the ankle (the stiffness of the system), as set by the central nervous system, sufficient to maintain upright stance. The authors prefer this to active control models (pinned polymer, stabilograms), as reaction time delays between COM motion and COP correction are not seen. In strictly reactive postural control, a reaction delay on the order of 100 ms would be expected due to central nervous system processing times. The conclusion is made that muscle stiffness set at the ankle and the inverted pendulum model are the best explanations for the observed data.

Morasso and Schieppati (1999) provide criticism of the model, as well as alternate explanations for some of the observed data. Referring to Figure 2.6, which is an alternate representation of the IP model to that displayed in Figure 2.5, the system equation is:

$$I_p\ddot{\theta} = mgh\sin(\theta) + \tau_a + z \tag{2.23}$$

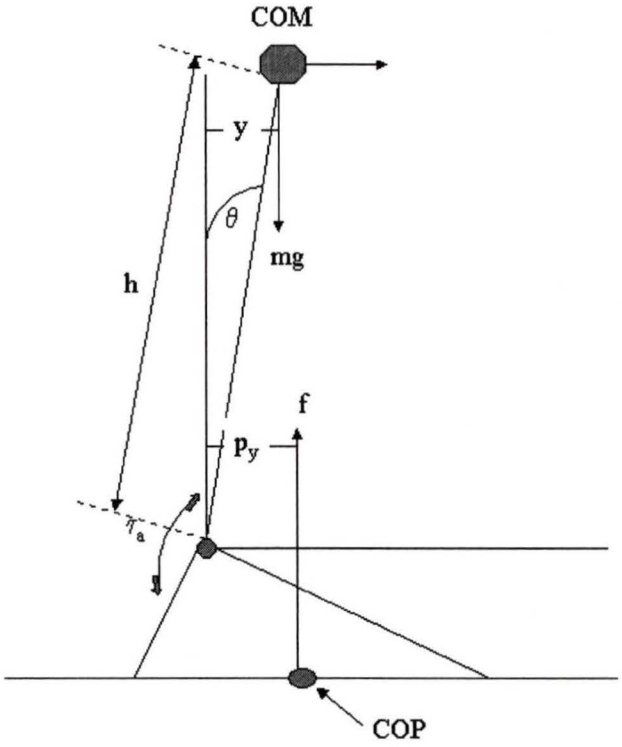

Figure 2.6: Diagram shows the forces acting on the postural system in the inverted pendulum model (Morasso and Schieppati, 1999).

where θ is the angle of sway, m is the mass of the body above the ankle, I_p is the inertia of the body above the ankle, h is the distance from the COM to the ankle, and τ_a is the total ankle-torque. z is the set of perturbations unrelated to postural control, such as respiration. The ankle-torque also is involved in the equilibrium equation for the foot, namely $\tau_a + f_v p_y \approx 0$,

where f_v is the vertical component of the ground reaction force, and p_y is again COP displacement. Several approximations can be used due to quiet stance: $f_v \approx mg$, $\sin\theta \approx \theta$ and $\ddot{\theta} \approx \ddot{y}/h$. Combining the foot and pendulum equation along with these approximations yields

$$\ddot{y} = \frac{g}{h_e}(y - p_y) + \frac{z}{mh_e} \tag{2.24}$$

where h_e is the "effective" height, defined as $h \times k_s$, where k_s is a shape factor for the inverted pendulum. For a uniform rod, $k_s = 1$, while if all mass was located at the COM, $k_s = 1.33$. For the human body, k_s lies somewhere between these two extremes, although closer to the first case.

In physical terms, (2.24) tells us that the COP-COM difference must be approximately proportional to COM acceleration, regardless of the control system that accomplishes this, because the postural noise is small in quiet stance. (2.24) also allows us to say that the horizontal component of the ground reaction force, f_H, must be proportional to $y - p_y$, as $f_H = m\ddot{y}$ by Newton's law. This leads the authors to the conclusion that," ... *although no specific receptors exist that detect the COM, its position y can be indirectly estimated through measurements of u [p_y] and f_H and some computational process that "fuses" them*"(p 1623). This is not in direct contradiction to the findings in Winter et al. (1998), but it means that the in-phase behaviour of the COP and COM cannot be used to justify a particular control scheme of the inverted pendulum model as claimed by Winter et al (1998). Similarly, the out-of-phase relationship of the COM (p_y) and the acceleration of the

COP ($\ddot{y}$) cannot be used to justify the control system; this property is again a physical necessity of the model. Letting A_y, Φ_y, A_p and Φ_p be the amplitude and phase parameters of y and p_y respectively, $\Phi_{\ddot{y}} = \Phi_{y-p_y}$ is always 180^0 out of phase with Φ_y by equation (2.16). This also implies that $\Phi_y = \Phi_p$, that the COM and COP are in phase with one another. Further, it is implied that $A_p > A_y$, as if the phase parameter of $y - p_y$ is 180^0 out of phase with the phase parameter of y, the amplitude component of p_y must be dominating the term.

An important observation here is that (2.24) provides a possible method for the calculation of the COM without having to measure it directly. Integrating (2.24) considering $p_y(t)$ as the forcing input (COP position controls the COM) accomplishes this. This makes it possible to collect the COP and calculate the COM position without the need for a three-dimensional tracking system.

This estimation of a COM from a COP trajectory is done using B-spline functions. Ignoring the noise component of (2.24) and solving for p_y yields

$$p_y = y - \frac{h_e}{g}\ddot{y}. \tag{2.25}$$

B-splines are sets of polynomials which provide a linearly independent basis for time (MacNab and Dean, 2001) in this case from 0 to 30 seconds. p_y is estimated from the splines using standard least squares methods, using a spline-estimated version of the right hand side of 2.25; B-splines are used

in place of y and $\ddot{y}$ as follows:

$$y(t) - \frac{h}{g}\ddot{y}(t) = [p_0(t) + p_1(t) + \ldots + p_B(t)] - \frac{h}{g}[\ddot{p}_0(t) + \ddot{p}_1(t) + \ldots + \ddot{p}_B(t)]. \tag{2.26}$$

The $p_i(t)$ are polynomials of a chosen order, with i running from 0 to B, the number of polynomials chosen to be in the basis. The coefficients from the best-fit regression model are then used to estimate y, the displacement of the COM. This method is alluded to in Morasso and Schieppati (1999).

The stability of the inverted pendulum system (as represented by (2.24)) is analysed through the use of Laplace transforms and transfer functions. Transfer functions are functions which define the relationship between the original space and the transformed space. They are present when converting a positional signal, such as a COP trajectory, into the frequency (Laplace) domain for further analysis. Using s as the Laplace transformed t, a Laplace transform on (2.24) yields the open loop transfer function:

$$Y(s) = \frac{1}{s^2 - g/h_e}\left[Z'(s) - g/h_e U(s)\right] \tag{2.27}$$

where $U(s)$ is the Laplace transform of p_y. $Y(s)$ can be shown to be unstable here, as one of the roots of the denominator $s^2 - g/h_e$ is positive (where $s = \sqrt{g/h_e}$). This means that for some real, achievable value, $Y(s)$ becomes infinite. The system can be stabilized by a proportional + derivative (P+D) feedback linear controller. This type of controller is used in many situations, such as regularizing singular systems in linear algebra (Chu et al., 1998), and

in non-linear systems (Flugge-Lotz and Taylor, 1956). A system with a P+D is made aware of where it is and the velocity with which it is moving. This reduces the magnitude of overcorrection errors which would be made by a control system with only positional information. Defining p_y (the controlling variable) $= K_p y + K_d \dot{y}$ with P+D gain factors gives a Laplace transform of

$$U(s) = (K_p + sK_d) Y(s). \tag{2.28}$$

Combining (2.27) and (2.28) makes Y(s) a closed loop transfer function defined by

$$Y(s) = \frac{1}{s^2 + (K_d s g)/h_e + (g/h_e)(K_p - 1)} Z'(s). \tag{2.29}$$

The roots of the denominator are now a pair of complex conjugate roots with negative real parts if the proportional gain of the controller, K_p, is larger than one. The response of the model to perturbations is one of damped oscillations. The natural frequency f_n and the damping coefficient ζ can now be computed as: $f_n = (1/2\pi)\sqrt{(g/h_e)(K_p - 1)}$ and $\zeta = (K_d/2)\sqrt{(g/h_e)(K_p - 1)}$. These parameters have already been estimated in the literature (Morasso and Schieppati, 1999). Typical values of $f_n = 0.5$ Hz and $\zeta = 0.2$ give $K_p \approx 2.01$ and $K_d \approx 0.127$ (given a typical h_e of 1.00 m). For almost any reasonable range of f_n and ζ, K_p remains above one, and thus the system appears to be stable. Simulations were run which verified that under suitably small perturbations (from $z(t)$) the system is indeed stable. This analysis shows that a simple feedback system is enough to maintain upright

stance, although it does not rule out more complex non-linear effects. These results lead to two physiological conclusions about balance. K_p >1 means the COP position must stay "ahead" of the COM position. K_d >0 means the anticipation of the COP must be greater when the COM is moving away from relative equilibrium and smaller if it is moving towards relative equilibrium. These conclusions do not reveal which type of postural control system is present (passive as in Winter (1998) or active). Both types of systems can be reconciled to the model. The passive system proposed by Winter et al. can only work, however, if the muscle stiffness set at the ankle can be high enough to provide sufficient stabilization.

If the stiffness control system is valid, the parameters of the control law above can be associated to the elastic and damping coefficients of the ankle joint. By a change of coordinates from y to θ, the elastic parameter K_p is related to K_a, the measurable ankle stiffness, by

$$K_a = mgh + I_p\,(K_p - 1)\,g/h_e. \tag{2.30}$$

Since the system must be stable, the minimum possible value of ankle stiffness occurs at $K_p = 1$. This means that K_a must be equal to mgh. For a "typical" subject, m = 80 kg, h = 1m. This gives a K_a of 784.5 N. Since the system does oscillate, the value must be greater than this (with $K_p = 1$, the system remains upright only if no movements occur). A more reasonable estimate of a necessary value can be found when f_n = 0.5 Hz, m = 80kg, I_p = 107 kgm^2, k_s (the shape parameter) = 1, K_a takes on the value of 1840 N.

Can the ankle stiffness achieve such a high measure? Different measures from the literature are cited, none of which are nearly large enough to justify the stiffness control model. Direct measures of ankle stiffness during standing are not available, so there is a chance that it could be much higher. It is likely, however, that active balance mechanisms play a large role in postural control, which would mean that ankle stiffness need not be set to such a high level.

Reviewing the debate on the nature of postural control (active versus passive), the authors conclude that an active scheme is more likely. They posit a system where receptors in the body provide a, "*postural state vector* $x = [y, \dot{y}]^T$ obtained from the complex combination of a variety of sway-related sensory signals."(pg 1625). This information on position and velocity is the type of information their control model needed. Simulation of reactions show that a delay of 50ms in feedback is enough to cause balance to fail. This implies that the system is not primarily reactive, as reaction times are longer than 50ms. Instead, the authors suggest that a computational process is present in the CNS is finding the state vector and compensating for reaction delays with anticipatory actions. This means that balance adjustments in locations such as the ankle would not be made to correct for the current state of balance, instead they would be made to prevent catastrophic failure of the system (falling, stepping) that would occur if current movements were not halted quickly enough.

The Inverted Pendulum Model seems to be useful for modeling the postural control system. The stiffness of the system, K, can be directly interpreted

as the muscle stiffness of a subject. This measure is useful clinically and also very difficult to measure directly during activity such as standing; standard tests measure muscle stiffness during rest. The method for estimating the COM proposed by Morasso and Schieppati is also very useful, should it be found reliable. Testing of their method could be done if data has been directly collected on both the COM and the COP. Drawbacks of the model include assuming that the ankles in the AP direction act in unison, as well as assuming postural adjustments are made only at the ankle. Observations have shown that (Shumway-Cook and Woollacott, 2000) there are two prominent balance strategies. The first is flexing at the ankle, while the second involves bending at the hips. The IP only models one of these accurately, although some results may still be applicable.

2.5 FARIMA Models

Sabatini (2000) used a fractional autoregressive integrated moving average (FARIMA) model to describe postural sway. The choice of this model indicates several assumptions made about the structure of the data. COP trajectories are viewed as self-similar, anti-persistent random walk processes. The process is, "... *obtained by fractionally summating the non-Gaussian random variable, whose correlation structure for small time lags is shaped by a linear time-invariant low-pass filter*" (Sabatini 2000). This is similar to the stabilogram-diffusion analysis; the FARIMA model, however, is not based on the assumption of Gaussian white noise underlying the system. Many different parameters are associated with this modelling process, including a Hurst exponent, as in the S-D analysis.

FARIMA models were introduced in 1981 by J. R. M. Hosking and applied to time series data. The purpose of FARIMA models is to provide a model family capable of modelling long-term persistence as well as explaining long and short-term correlations in data. FARIMA models are an extension of ARIMA (autoregressive integrated moving average) models, as introduced by Box and Jenkins (1976).

Using {-} to denote a time series, an ARIMA$(0,1,0)$ process $\{x_t\}$ is the discrete time analogue of Brownian motion, defined as

$$\nabla x_t = (1 - B)\, x_t = a_t \tag{2.31}$$

where B is the backward shift operator defined as $Bx_t = x_{t-1}$ and the a_t

are independent identically distributed random variables. $\{a_t\}$ is the first difference of $\{x_t\}$ with $a_t = x_t - x_{t-1}$; $\{a_t\}$ is also a white noise process. Fractional differences can also be explored. Where d can take on any real value, defining ∇^d as the fractional difference operator through the binomial series expansion,

$$\nabla^d = (1-B)^d = \sum_{j=0}^{\infty} \begin{pmatrix} d \\ j \end{pmatrix} (-B)^j \tag{2.32}$$

a series$\{x_t\}$ is a FARIMA$(0, d, 0)$ process if $\nabla^d x_t = a_t$, where $\{a_t\}$ is again a white noise process. The reverse relationship also holds, i.e.,

$$\nabla^{-d} a_t = x_t \tag{2.33}$$

Note that d is directly related to the Hurst exponent from Fractional Brownian motion by the relationship $d = H - 1/2$. The x_t are defined as a moving average of the a_t in this way. $\{x_t\}$ has several properties which can be derived (see Hosking, 1981) from the definition of the process:

1. When $d < 1/2$, $\{x_t\}$ is a stationary process which can be expressed as an infinite moving average (MA)

$$x_t = \psi(B) a_t = \sum_{i=0}^{\infty} \psi_i a_{t-i} \tag{2.34}$$

where

$$\psi_i = \frac{(i+d-1)}{i!\,(d-1)!} \tag{2.35}$$

2. When $d > 1/2$, $\{x_t\}$ is invertible and has infinite autoregressive representation

$$\pi(B)\, x_t = \sum_{i=0}^{\infty} \pi_i x_{t-i} = a_t \tag{2.36}$$

where

$$\pi_i = \frac{(i-d-1)}{i!\,(-d-1)!} \tag{2.37}$$

3. $\{x_t\}$ has spectral density $s(\omega) = [2\sin(\omega/2)]^{-2d}$ for $0 < \omega \leq \pi$.

4. $\{x_t\}$ has covariance function

$$\gamma_i = \frac{(-1)^i\,(-2d)!}{(i-d)!\,(-i-d)!} \tag{2.38}$$

FARIMA$(0, d, 0)$ processes have many other properties as well (Hosking, 1981). One important note is that such a process, "*...may be summed or differenced a finite integral number of times until d lies in the interval* $[-1/2, 1/2]$ *and will then be stationary and invertible...*"(pg 169, Hosking). This property is not as strong where $d = \pm 1/2$, where the final process is either stationary or invertible but not both. This makes $[-1/2, 1/2]$ the most useful range of d values as other FARIMA$(0, d, 0)$ processes, with d values outside of that range, may be transformed through a MA operation until the d of the transformed process lies in $[1/2, -1/2]$.

A further generalization of FARIMA models is possible, to FARIMA (p, d, q) models. These models are defined as follows, where p and q must be

integers:

$$x_i - \sum_{j=1}^{p} \varphi_j x_{i-j} = \sum_{k=0}^{q} \theta_k \nabla^{-d} a_{i-k}. \tag{2.39}$$

The φ_j are the autoregressive (AR) coefficients of the model, and the θ_k are the MA coefficients. The AR and MA parts of the model allow for the modeling of short time lag structure, as the main purpose of d is to describe the long time lag structure. As shown in Hosking, the long-term behaviour of a FARIMA$(0, d, 0)$ and a FARIMA(p, d, q) are similar no matter the values of p and q. This is because the effects of p and q decay exponentially, while the effect of d decays only hyperbolically. This type of model seems ideal to explain COP trajectories; as was shown during the S-D analysis, the correlation structure of COP trajectories shows different short and long-term behaviours.

Sabatini decided to model COP trajectories using the FARIMA(p, d, q) approach. This model was chosen after an examination of other possible modeling techniques, such as stabilograms. The first test run on the COP trajectories was one of self-similarity. A continuous time process $\{y(t)\}$ is self-similar if for some self-similarity parameter H (the Hurst exponent),

$$Y(t) \stackrel{d}{=} c^{-H} Y(ct) \quad \forall t > 0, \forall c > 0, 0 < H < 1, \tag{2.40}$$

equality here is in distribution. Fractional Brownian motion, for example, is self-similar. Assessing distributional equality is difficult in practice, so

self-similarity is often assessed using absolute moments, defined as

$$\mu^{(m)}(r) = E\left[\left|X^{(m)}\right|^{(r)}\right] \tag{2.41}$$

where $X^{(m)}$ is called the *aggregated sequence* with aggregation level m. "*Its samples are constructed by dividing the (stationary) increment process* $X = \{X_i, i \geq 1\}$ *of* Y *into nonoverlapping blocks of size* m..." (Sabatini, p. 1226). Averaging over blocks gives

$$X_k^{(m)} = \frac{1}{m} \sum_{i=(k-1)m+1}^{km} X_i, k = 1, 2, ... \tag{2.42}$$

If X is self-similar, then

$$\log \mu^{(m)}(r) = \beta(r) \log m + \alpha(r) \tag{2.43}$$

where $\beta(r)$ is linear with respect to r, $\beta(r) = r(H\text{-}1)$. It is the absence or presence of this linearity which decides the outcome of the test. In practice, sample absolute moments

$$\hat{\mu}^{(m)}(r) = \frac{1}{N/m} \sum_{k=1}^{n/m} \left|X_k^{(m)}\right|^r \tag{2.44}$$

are used in place of the true moments. Self-similarity testing is done on the COP trajectories on the time lag regions from 1 to 10 seconds. This was done to prevent under- or over-sampling, both of which can distort the results of the testing. This time range gives $100 \leq m \leq 1000$. r was tested in the range of $(1, 4)$; non-integral moments are included in the testing. Using (2.43) and the properties of $\beta(r)$, an estimate of $H(r)$ (and through that an estimate of

$d = H$ - $1/2$) can be found by fitting in log-log space. Estimates of H should be more or less constant over different values of r. This is confirmed for the COP data analysed, with variations in the H estimate, "... *comparable in size to the fluctuations affecting the estimates of the Hurst exponent*" (Sabatini, 2000). Sabatini (2000, p. 1222) displays a typical result from this procedure as applied to COP data. The results in Sabatini (2000) are taken as sufficient evidence that COP trajectories may be viewed as coming from a self-similar model. This conclusion is dependent on the assumptions that for short time-lags (aggregation levels under $m = 100$) the estimates one gets from a self-similar analysis are largely due to data over-sampling and short-range effects. The short-range effects are,"... *due to the action of a low-pass filter applied to a self-similar random process with Hurst exponent* $H = H_l$" (Sabatini, 2000) (the l subscript indicates long-range). This contrasts with S-D analysis, which treats the short and long-term effects as equally important.

Once the appropriateness of the FARIMA(p, d, q) model has been established, the next step is to estimate p, d, and q. A key feature of the method proposed by Sabatini (2000) is the estimation of d separately from the other two parameters using Peng's method (Peng et al., 1993).

Peng's method is a way of estimating the Hurst exponent of a time series. The method is graphical, and is robust to non-normality. The method used is very similar to that used in stabilogram-diffusion plots. With the x_i defined as the movements generated from a FARIMA model (as in (2.34)), the measured

position COP_v of the COP after v time-steps is

$$COP_v = \sum_{i=1}^{v} x_i. \tag{2.45}$$

Now define the difference $d_w(v)$ over a time interval w as $d_w(v) = COP_{v+w} - COP_v$. The root mean square fluctuation of the d_w is

$$\langle d_w^2 \rangle = \sum_{v=1}^{10} \frac{d_w(v)^2}{n} = C_w = \sqrt{\langle d_w^2 \rangle - (\langle d_w \rangle)^2}, \tag{2.46}$$

where n is the number of points in the average. The averaging indicated by $\langle\rangle$ takes place over v, in this case from 1 to 10 seconds by increments of 0.01, giving an n of 901. As in the S-D plots, an estimate of D is the slope of the log-log plot of C_w against w. This D is also an estimate of the Hurst exponent H. The main difference between this method and the S-D method is that here the slope estimation is done over a pre-defined region of 1 to 10 seconds time-lag, not from a user-estimated cut-off region to 10 s. Estimates of H are also done in Peng's method on each trial, whereas the S-D method averaged the stabilograms of each trial prior to estimation. The short-range H is not estimated here due to the assumed dominance of short-range effects.

Once the estimate of H has been found, this allows the construction of a MA operator to remove the fractional component of the data. H is related to the d as before, $d = H - 1/2$. Properly defining the MA operators should (assuming a good estimate of H), once applying them to the data, yield an autoregressive moving average (ARMA) signal. The coefficients of the MA

as defined in Sabatini (2000) are

$$h_0 = 1, h_i = (i - 1 - d)\frac{h_{i-1}}{i}. \tag{2.47}$$

Once the data has been reduced to an ARMA process, standard techniques and measures are available to describe it once the order of the process has been identified. Sabatini (2000) used MATLAB algorithms to determine the number of autoregressive terms which provided the best fit to the data. Further measures on the system, DC Gain, Natural Frequency, and Damping Ratio, are also extracted using MATLAB routines (Sabatini, 2000). These parameters are measures of a system that can be defined by a transfer function such as an ARMA signal, and are produced by Sabatini (2000) without details. DC gain is defined as, "*...the final value of the system response to a unit step input*"(Mutambara, 1999). It is a unitless quantity. The natural frequency corresponds to the frequency the system would oscillate at if no damping was present (Hale, 1988); it has units of radians per second, or can be converted to Hertz as well. The damping ratio controls the rate at which oscillations in the system would die down given no further perturbations. Dimensionless, a damping ratio of 0 means the system will oscillate forever, and a damping ratio of 1 indicates a system's response to a perturbation will return it to equilibrium without any overshoot. Typical values of the damping ratio lie between these two extremes, giving corrections to perturbation that will oscillate in a decreasing manner about the equilibrium position (Hale, 1988).

Other tests were also applied to the data. Hinich's test for normality was applied to the COP increments, which are the differences between subsequent points in a COP trajectory. This involves a best fit of the data to a symmetrical Lévy stable PDF with parameters α and γ

$$p(x;\alpha,\gamma) = \frac{1}{\pi}\int_0^\infty \exp(-\gamma q^\alpha)\cos(qx)\,dq. \tag{2.48}$$

The normal distribution is parameterized by Lévy's distribution with $\alpha = 2$. A departure from normality would contradict the underlying assumption of normality used by many models. The run-test for stationarity in mean and variance was also applied to the COP trajectories.

The data under analysis in Sabatini (2000) came from a group of ten healthy adults, five male and five female. All subjects had no known balance problems. Twenty trials were performed on each subject, ten with eyes open fixed on a visual reference, ten with eyes closed. All trials were performed in a relaxed stance position on an AMTI force platform, for a duration of 60 seconds, at a collection rate of 100 Hz. As with prior studies, the A/P and M/L components of the COP trajectory were extracted and analysed separately. The first ten seconds of each trial were discarded to avoid transient data effects, as demonstrated by Figure 2.1. After the initial fractional differencing procedure, referred to by Sabatini (2000) as "*fractional deconvolution*", yielded an ARMA signal, the data was filtered with an FIR filter, and down-sampled by a factor of ten, leaving a time series composed of 500 samples. The frequency components of the COP fluctuations are less than 5

Hz, so this down-sampling does not affect the interesting signal components. It is done to reduce over-sampling and noise levels.

The run-test (Bendat and Piersol, 1993) for stationarity (at $p < 0.05$) confirmed stationarity in mean in 99% of the trials, variance in 95% of the trials. Results did not depend on stance (EO, EC) conditions. A small oscillation at 0.2-0.3 Hz, most likely respiration, was often detected; Fisher's test (D'Agostino et al., 1988) applied to single periodic components from the periodogram rejected the null hypothesis of no periodicity (at $p < 0.05$) in 33% of the trials. These results imply that non-stationarity detected in COP data is due to the nature of the random walk, not an intrinsic change of the data. Hinich's test showed the best fit α to be approximately 1.70 ± 0.18 (mean $\pm$ SD). This was a consistent result over both stance conditions. From this, it was concluded that the COP increments are not normally distributed.

The strength of the stochastic driving, which Sabatini defines as the root-mean square of the COP increments (essentially measuring the variation of the COP increments), revealed the presence of two groups within the ten subjects, each of size five. These groups are differentiated by the existence or non-existence of a change in the Hurst exponent estimate (calculated as detailed above) in the M/L direction between the EO and EC conditions. Similar groups were previously seen in stabilogram-diffusion analysis (Collins, De Luca, 1995). The groups show similar Hurst exponents under EC conditions, but under EO conditions, group 1 show higher H estimates. Results are summarized in Table 2.5. These differences are only significant in the eyes open, A/P data.

Hurst Exponents	**EO-ML**	**EC-ML**	**EO-AP**	**EC-AP**
Group 1 mean ± SD	0.18 ± 0.11	0.10 ± 0.11	0.33 ± 0.09	0.13 ± 0.09
Group 2 mean ± SD	0.11 ± 0.08	0.09 ± 0.12	0.20 ± 0.12	0.14 ± 0.12

Table 2: A summary of Sabatini's findings with respect to changes in Hurst exponent estimates.

Fitting the FARIMA model yielded a FARIMA(4,d,0) model as the best fit, with the value of d determined by the individual subject. This model provides the lowest final prediction error (FPE), with an average value of 0.28. Fitting just an ARIMA(p,q) model to the data gave a best fit as ARIMA(4,0), with an FPE averaging 0.46. That the FPE is lower when the data has been deconvolved supports the hypothesis that the data can be modelled better as fractionally differenced. Once the best-fit model was determined, three further parameters were extracted from the model, DC Gain, Natural Frequency, and Damping Ratio. These parameters are associated with the fractionally deconvolved, filtered, and down-sampled data. Comparing the EO and EC conditions, it is shown that the DC gain and damping ratio both tend to be higher under EC conditions; a slight decrease in the natural frequency is seen. Significant differences between EO and EC exist for all three measures in both directions for group 1; for group 2, only the increase in damping ratio in the ML direction is significant. The same trends are seen for each group and stance direction for each of the measures.

A different weighting of the balance sensory inputs is hypothesized to explain the existence of two groups. Under EO conditions, the balance system

is less strongly correlated, particularly for group 1 subjects. This implies that visual input is reducing the feedback of the proprioceptive and vestibular systems. This does not, however, lead to a wider range of motion. Removing the visual inputs and observing an increase in DC gain is said to imply, "*... that the musculoskeletal system, in particular the ankle, has the highest impedance when the balance task is more demanding...*" (Sabatini, 2000). This is more evident in the A/P direction as the body is more stable in the M/L direction. Sabatini also states that the lower natural frequency and high DC Gain of the system under EC conditions support the idea of a more conservative balance control strategy when visual input is removed.

The main idea put forth by Sabatini (2000) is that the behaviour of the S-D plots can be explained not by an open/closed-loop dual control system, but rather by modelling the data as a self-similar anti-persistent random process. This analysis is almost certainly better than the S-D analysis, as it avoids making assumptions about the structure of the data, instead relying on testing for the structure. While the FARIMA approach does produce several outputs that seem descriptive, it does not produce an output with the direct interpretability of the K values seen in the PP model or the K_e values from the IP model. This limits its immediate clinical use, although it may point the way toward more detailed modelling in the future.

Chapter 3

Model Implementation and Results

3.1 Descriptive Measures

3.1.1 Implementation of the Descriptive Measures

The software accompanying the AMTI platform was used to obtain descriptive measures on COP trajectories. Measures recorded from this source were velocity, 95% ellipse area, x-range, and y-range. Accuracy of these measures were verified by independent calculations on the same data sets using SPLUS (although problems do exist with formulae given in the AMTI force plate manual). X-range is defined as the maximum value of the M/L component of a COP trajectory minus the minimum value of the M/L component. Y-range is defined in the same way, except with respect to the A/P compo-

nent of a COP trajectory. Velocity can be calculated as the total distance travelled by the COP trajectory divided by the duration of the trajectory. The total distance travelled is the sum of the distances from one point to the next, with the velocity defined as follows:

$$Velocity = \frac{1}{30seconds} \sum_{i=1}^{N-1} \sqrt{(x_{i+1} - x_i)^2 + (y_{i+1} - y_i)^2}. \tag{3.1}$$

The 95% area ellipse measure is derived as follows. The half lengths of the major (longest) and minor (shortest) axes of the ellipse are equal to

$$\begin{aligned} l_{major} &= \sqrt{\lambda_1} \times \sqrt{\chi^2_{0.05,2}} \\ l_{minor} &= \sqrt{\lambda_2} \times \sqrt{\chi^2_{0.05,2}} \end{aligned} \tag{3.2}$$

where λ_1 and λ_2 are the eigenvalues of the covariance matrix of the COP trajectory, and $\chi^2_{0.05,2} = 5.99$ is the 95% critical value resulting from an assumption of bivariate normality (Rencher et al., 1995). The area of the 95% ellipse is given by the equation for the area of an ellipse, in terms of the two axes,

$$Area = \pi \times l_{major} \times l_{minor}. \tag{3.3}$$

The 95% ellipse area is based on a multivariate 95% acceptance region centered at the origin (because the data is normalized to be centered there). A point falling outside the region is one where the null hypothesis would be rejected. The null hypothesis in this case is that the point came from the bivariate normal distribution specified by mean vector [0,0] and the covariance matrix mentioned above.

Previous studies that have tested for significant differences between conditions and groups using measures estimated by COP data have done so using various statistical testing methods, including Mann-Whitney testing (Viitasalo et al., 2002), modified z-tests (Diener et al., 1984), ANOVA (Nardone et al., 2001, Hunter and Hoffman, 2001) and regression (Maylor and Wing, 1996). As the effect of trial is also under investigation in this study, these methods are insufficient. With this study, we wished to detect effects which take place over the course of trials. These effects may be caused by subject learning or fatigue. Using the data collected as described above, the four descriptive measures velocity, 95% ellipse area, x-range and y-range were fit as the dependent variable in a GEE (generalized estimating equation) model (Diggle, Liang and Zeger, 1999) with SAS. The independent variables used were subject group (DS or non-DS), vision condition (EO or EC), and trial (from 1 to 10 for each set of trials done under each vision condition). Two and three-way interaction terms were also included in each model. SAS code for this fit is given in Appendix A.2.

The main benefit of GEE models is their flexibility for data with repeated measures, such as the data in this study. GEE models provide an estimate of the effect of each term in the model through its coefficient, much like a simple linear regression. These coefficients are estimated through a quasi-likelihood procedure. Given a reasonable estimate for the variance-covariance structure of the data, GEE models give nearly efficient estimates relative to maximum likelihood estimates (mle's) (Diggle et al.,1999). GEE models can accommodate many variance-covariance structures. They are also robust to departures

from the assumed nature of these structures. Since the true likelihood structure of this type of data is not usually known, it is not generally practical to pursue mle's. Furthermore, residual analysis can reveal problems which may have occurred in the fitting process. Residual analyses of the GEE models fit showed no notable problems.

3.1.2 Results from the Descriptive Measures

The summary of the descriptive measures are given in Table 3.1, split by DS vs non-DS subjects and the EO/EC conditions. Comparing the subject groups under the same visual conditions, the DS group has higher mean in each case. DS subjects also have higher standard deviations for each measure. Further examination of these trends was done through the use of GEE models. Results from the GEE models fit to the descriptive measures are given in Table 3.2.

For 95% ellipse area, there is a marginally significant difference between the EO and EC conditions (p=0.07) indicating an increase in area under the EC condition. There is no significant difference between the DS and non-DS subjects.

Velocity shows a significant difference between DS and non-DS subjects (p=0.002), with DS having higher velocities. There are also significant differences between EO and EC (p=0.03), with an increase in velocity under EC conditions.

X-Range shows a significant trial effect (p=0.05). There are significant

differences between EO and EC (p=0.003) and a significant interaction between EO/EC and trial (p=0.02).

Y-Range shows a significant difference only between the EO and EC condition (p=0.045), indicating larger y-range under the EC condition.

All of the descriptive measures show a significant difference between the EO and EC conditions. This is not unexpected, given similar results in other studies examining these measures (Diener et al., 1984, Viitasalo et al., 2002). Average velocity is the only descriptive measure that differentiated the DS and non-DS groups. This is consistent with previous studies in this area (Vuillerme et al. 2001, Vieregge et al. 1996), which showed that velocity is the best descriptive measure with which to detect differences between DS and non-DS subjects. There could, however, be several reasons for an increase in the COP's velocity. One possible reason is an increase in the stiffness of a subject, which would cause faster movements, although not necessarily ones that cover a greater range. The PP and IP models attempt to determine the stiffness of a subject, and hence allow us to evaluate whether a stiffness change may be causing observed differences between subject groups.

Eyes Open	Average 95% Ellipse Area (cm^2)	Average Velocity (cm/s)	Average X-Range (cm)	Average Y-Range (cm)
DS Subjects	4.024 (±2.287) 1.974 – 8.469 [0.56 – 14.47]	2.000 (±0.511) 1.338 – 2.753 [1.12 – 5.17]	2.267 (±0.522) 1.699 – 3.054 [0.76 – 5.28]	2.643 (±0.886) 1.739 – 4.152 [0.98 – 5.94]
Non-DS Subjects	2.449 (±1.126) 1.097 – 4.774 [0.60 – 7.08]	1.422 (±0.188) 1.230 – 1.794 [1.05 – 2.25]	1.705 (±0.386) 1.040 – 2.103 [0.76 – 3.26]	2.053 (±0.551) 1.326 – 3.153 [0.84 – 5.82]

Eyes Closed	Average 95% Ellipse Area (cm^2)	Average Velocity (cm/s)	Average X-Range (cm)	Average Y-Range (cm)
DS Subjects	3.745 (±1.651) 1.542 – 5.757 [0.83 – 13.45]	2.373 (±0.803) 1.615 – 4.225 [1.41 - 5.90]	2.244 (±0.522) 1.316 – 2.812 [0.83 – 4.84]	2.715 (±0.695) 1.674 – 3.591 [1.13 – 5.20]
Non-DS Subjects	3.469 (±1.511) 1.846 – 5.948 [0.79 – 10.40]	1.580 (±0.236) 1.272 – 1.958 [1.10 – 2.41]	2.020 (±0.511) 1.375 – 2.961 [0.84 – 3.98]	2.527 (±0.482) 1.960 – 3.276 [1.07 – 4.85]

Table 3.1: Summary statistics for each of the descriptive measures taken from the COP trajectories. Results are subdivided into sub-tables for the EO/EC conditions, and tabulated by DS versus non-DS. The averages of the subject averages over ten trials (± standard deviations of the subject averages over ten trials in the second row) are shown in the first row of each cell. The third row of each cell contains the minimum and maximum values of the subject averages over trials, and the last row contains the minimum and maximum values over all measurements taken of the given category.

GEE Results	Trial	DS	EO/EC	Trial × DS	Trial × EO/EC	DS × EO/EC	Trial × DS × EO/EC
95% Area (cm^2)	0.03 (0.04) 0.48	0.85 (0.63) 0.17	**1.14** **(0.63)** **0.07**	0.13 (0.09) 0.15	-0.03 (0.06) 0.72	-0.97 (0.84) 0.25	-0.06 (0.13) 0.63
Velocity (cm/s)	0.002 (0.007) 0.76	**0.56** **(0.18)** **0.002**	**0.17** **(0.08)** **0.03**	0.0043 (0.017) 0.79	-0.003 (0.006) 0.58	0.25 (0.32) 0.43	-0.007 (0.03) 0.84
X-Range (cm)	**0.027** **(0.014)** **0.05**	0.32 (0.22) 0.15	**0.58** **(0.2)** **0.003**	0.045 (0.044) 0.30	**-0.049** **(0.02)** **0.02**	-0.5 (0.32) 0.12	0.03 (0.054) 0.59
Y-Range (cm)	0.0008 (0.012) 0.95	0.53 (0.34) 0.12	**0.62** **(0.31)** **0.045**	0.012 (0.026) 0.63	-0.027 (0.029) 0.34	-0.52 (0.41) 0.21	0.021 (0.046) 0.64

Table 3.2: Results from a GEE model fit of the dependent variable (1^{st} column) versus the independent variables (1^{st} row). Within each cell are the coefficient estimates, the standard error in brackets, and the p-value for testing the hypothesis that the coefficient is zero. Significant or marginally significant p-values appear in bold.

3.2 The Pinned Polymer Model

3.2.1 Implementing the Pinned Polymer model

Implementing procedures to fit the Pinned Polymer model is quite challenging. Processing the data to obtain an individual or averaged normalized derivative of the autocorrelation function (henceforth these are referred to as INDA or ANDA) is a time consuming procedure. The first step in the data processing involves obtaining the autocorrelation function (ACF) for the A/P component of each COP trajectory. This is done using the *acf* function available in SPLUS. As specified within this function, the ACF is obtained for time lags from zero to nine seconds, or from 0 to 900 data points, as the data was collected at 100 Hz. The negative derivative (ND) of the resulting ACF is estimated using a simple first order difference, or $ND_i = y_i - y_{i+1}, i = 1, ..., 899$. The location and value of the maximum of the negative derivative are then found for normalization. The normalized version of the negative derivative is the negative derivative starting at the maximum location and divided through by the maximum value. This ensures that each INDA of the ACF begins at 1 and decreases from there, allowing future averaging of the INDA across the various trials.

Fitting a Bessel Function to INDAs or ANDAs is more challenging than computing them. Within the possible ranges of the data, there are four numerical approximations to the Bessel function (Press et al., 1990) which are implemented. The use of the approximations depends on the value being entered into the Bessel function as in (2.8). Real and imaginary values give

different approximation functions, as do values of greater magnitude as time increases through the data. Imaginary values occur where $4\alpha\beta < 1$, which is a reasonable range for the parameters. In the data examined here, for the ANDA under EO conditions, 8 of 19 subjects fell in this range of parameter values. Under EC conditions, this occurred in 5 of 19 subjects. Approximations were checked for accuracy and continuity before proceeding with the fitting procedure. The complex approximation structure of Bessel Functions makes it very difficult to apply standard optimization techniques. This lead Lauk et al. (1999) to use the Levenberg-Marquardt method to find optimal parameters, which is the method chosen in this study as well.

The L-M method is a steepest descent and inverse-Hessian algorithm that uses numerical and analytical information. It has "*...become the standard of nonlinear least-squares routines*" (p 524 Press et al., 1990). The L-M method computes estimates of the variance and Hessian matrices to be used in determining the best-fit model; the user does not need to provide general structures or preliminary estimates for the matrices. The variance matrix can also be used to estimate the variance of the parameter estimates from the best-fit model.

For full implementation, the method requires the derivatives of (2.8) and (2.9) with respect to each of α and β. Simplifying the completion of these derivatives are two properties of Bessel functions (Marsden, 1973)

$$J_n'(z) = \frac{1}{2}\left[J_{n-1}(z) - J_{n+1}(z)\right], \quad J_n(z) = (-1)^n J_{-n}(z) \quad . \tag{3.4}$$

Combining these two properties simplifies the derivative of the zero'th order Bessel function to

$$J_0'(z) = -J_1(z). \tag{3.5}$$

Assumptions are made about the form of the transformed data before implementation of the L-M method. The data are normalized to have a y-intercept at 1; variations in the intercept of the model are accomplished through changes in the v parameter of (2.8) and (2.9). Model selection was done initially with v as a parameter, which often yielded results that did not agree well visually with the initial segment of the data. It is this segment of the data to which it is most important to fit, as the initial drop of the Bessel function is determined by α and β, and hence determines K. It was decided therefore to hold v constant; v was assigned a value of $1/4\beta$ to ensure the best-fit model had a y-intercept at 1. Fitting was also done in this way in Lauk et al. (1999); the model is represented, as stated earlier by (2.11)

$$e^{-t/2\beta} J_o\left(\frac{\sqrt{4\alpha\beta - 1}}{2\beta} t\right). \tag{3.6}$$

From (3.5), it can be shown that the derivatives of (3.6) are, keeping in mind that v is constrained to be $1/4\beta$,

$$\frac{dR}{d\alpha} = -J_1\left(\frac{t\sqrt{4\alpha\beta - 1}}{2\beta}\right) e^{\frac{-t}{2\beta}} \frac{t}{\sqrt{4\alpha\beta - 1}},$$

and that

$$\frac{dR}{d\beta} = J_0\left(\frac{t\sqrt{4\alpha\beta-1}}{2\beta}\right)e^{\frac{-t}{2\beta}}\frac{t}{2\beta^2} - J_1\left(\frac{t\sqrt{4\alpha\beta-1}}{2\beta}\right)e^{\frac{-t}{2\beta}}t\frac{-2\alpha\beta+1}{2\beta^2\sqrt{4\alpha\beta-1}}. \tag{3.7}$$

Similar forms hold for the derivatives of (3.6) when I_0 is substituted for J_0. For the purposes of minimization, a χ^2 cost function was used of the form

$$X = \sum_{i=2}^{600}\left(\frac{\mu_i - c_i}{s_i}\right)^2 \tag{3.8}$$

where μ_i are the ANDA values for a single subject under a single visual condition, s_i are the sample standard deviation of the μ_i estimated from the INDA values, and c_i is the fitted model chosen by the L-M method. i runs from 2 to 600 here as fitting has been done over the first 600 points, or for a 6 second time lag. The first point is excluded as the estimated standard deviation is necessarily zero at the first point where all the trials have been normalized to 1. Where p is the number of parameters estimated in (3.8), X has an approximate χ^2 distribution with $n - p = 600 - 3 = 597$ degrees of freedom under the assumption that the errors in s are independently and identically distributed. This assumption is not met by the data, as the errors start out very small and become larger at later time lags. As it is desired to fit the initial part of the data more precisely, this statistic's heavier weighting there makes it useful. When fitting single trials, no s is available for (3.8), so one was assigned with a constant value. Other choices were explored, but for single trials, no marked improvement was seen when weighting the earlier

portions of the data more heavily.

The L-M method has many drawbacks which are evident when fitting the PP model. The first of these is a tendency to find a local minimum when not given proper initial values. This is not unexpected, as the L-M method is relatively simple to implement and follows a basic idea of error sum of squares minimization. Locating local minima which depend on the initial values of the parameters given to the searching algorithm does make automation extremely difficult to implement; in the case of this data, the range of possible values of α and β are extensive. As mentioned earlier, it is most important to have the correct ratio of α and β to ensure a proper fit. It is also vital to have the proper scale for α and β, i.e., using values of 1 and 1 for α and β yields a much different curve than using 5 and 5. As such, for an INDA or an ANDA, it is necessary to visually select a model (curve) which appears to be a good fit prior to using the L-M algorithm. Final values for most models depend most strongly on the initial values provided, and one must be cautious to try and find better fits even when one that has been done already appears to be sufficient. Very small improvements on most fits, in terms of X, may be possible to achieve through further sets of initial values. Proceeding in such a manner cannot continue for too long, however, as a second drawback of the L-M method is that it is not a computationally quick algorithm. These delays mean the process of finding a good fit can take several minutes for each trial. The number of cycles and improvements the algorithm is allowed to make was held to a minimum, with a variable available in the output to see if further cycles should be done. This variable

is an indicator that tells the user when the last model was chosen; if a new best-fit model has been chosen within the last two searches, further cycles are recommended (see Appendix A.4 for further details). While practice does improve the efficiency of the procedure for fitting the PP model, it remains the most time consuming aspect of the data analysis.

The estimates of K that result from the model fitting were analysed using a GEE model in the same way the descriptive measures were. The estimates of K had a skewed distribution, so to meet the assumption that the data should be distributed as approximately normal, the K values were log-transformed. This transformation yielded a reasonable approximation to normality.

3.2.2 Results from the Pinned Polymer Model

Starting with the results fitting to INDA's, referring to Table 3.3, K shows a marginally significant interaction between the EO/EC condition and the subject group (p=0.056). The DS $\log(K)$ estimates increase over trials at approximately the same rates for the EO and EC conditions. The estimates are larger under the EC condition. The $\log(K)$ estimates for the non-DS subjects increase over trials under the EC condition, but decrease over trials under the EO condition. Estimates under the EC condition are larger than under the EO conditions for both DS and non-DS. The DS estimates are larger than the non-DS estimates over both conditions and over all trials. These findings are summarized in Figure3.1.

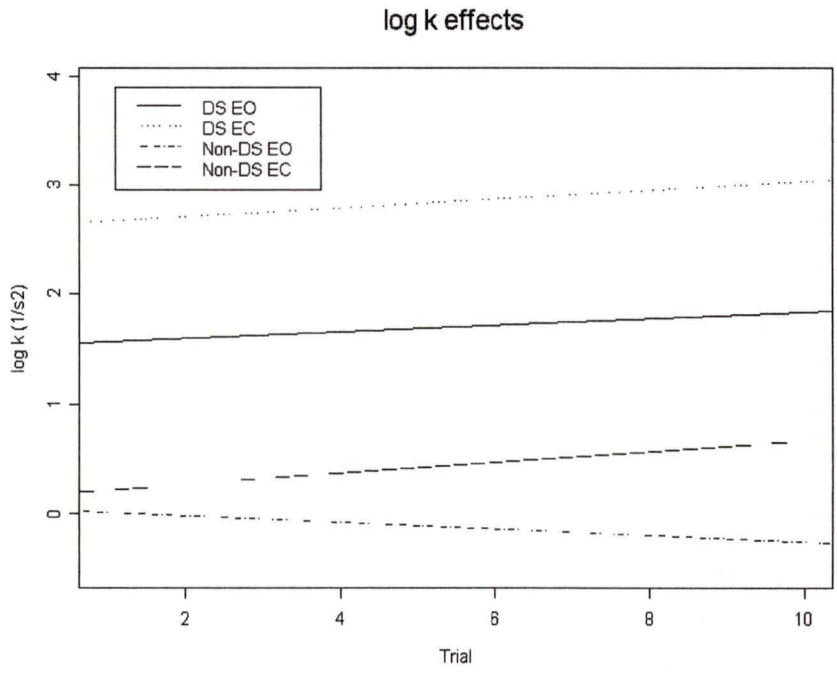

Figure 3.1: GEE model fitting results for $\log(K)$.Estimated values for each of the EO/EC and DS versus non-DS conditions are graphed versus trial number.

The ANDA analysis shows some of the same trends seen in the INDA analysis. The ANDA stiffness shows an increase under the EC condition for both groups, although this difference is non-significant (two-tailed t-test, p=0.11). DS subjects have significantly higher $\log(K)$'s than those of the non-DS group (two-tailed t-test p-value < 0.001). Table 3.4 displays the summary statistics for both INDA and ANDA $\log(K)$, as well as K_e.

GEE Results	Trial	DS	EO/EC	Trial × DS	Trial × EO/EC	DS × EO/EC	Trial × DS × EO/EC
K (PP) (s^{-2})	-0.031 (0.091) 0.73	**1.5** **(0.7)** **0.032**	0.13 (0.34) 0.79	0.058 (0.095) 0.54	0.075 (0.01) 0.46	**0.96** **(0.5)** **0.056**	-0.058 (0.11) 0.59

Table 3.3: Results from a GEE model fit of $\log(K)$ versus the independent variables. Within each cell are the coefficient estimates, the standard error in brackets, and the p-value for testing the hypothesis that the coefficient is zero. Significant or marginally significant p-values appear in bold.

The X statistics for the individual trial fits ranged from a low of 3.04 to a high of 62.6 under the EO condition, and from 3.1 to 37.6 with EC. A value of over 20 generally indicated a poor fit to the entire length of the data, with a significant number of trials falling into this range. 34 trials (24 non-DS, 10 DS) of a total of 179 under the EO condition fell in this range, and 35 (29 non-DS, 6 DS) of 178 total fell in this range under the EC condition. Note that three trials had collection problems, which limited the total trials to 377 instead of 380. Some individuals did show a tendency to particularly bad fits, with subject 4 (a non-DS subject) having 14 of 20 trials showing an X above 20.

The X statistics for the ANDA ranged from 86 to 2880. Assuming a χ^2 distribution, a 99% region for the null hypothesis that the model fit the data is at 681. 5 out of 36 ANDA fits fell outside of this range, with 2 under EO and 3 under EC conditions, and 2 for non-DS and 3 for DS subjects. Subject 13 (DS) exceeded 681 under both eye conditions, and also had the highest value observed at 2880. The use of the χ^2 distribution for the X statistics is

Eyes Open	ANDA log K (PP)($1/s^2$)	INDA log K (PP) ($1/s^2$)	K_e (IP) (N*m/rad)
DS Subjects	0.653 (±0.559) -0.201 - 1.545	1.685 (±1.150) 0.370 - 3.822 [-3.266 - 4.948]	1260.9 (±544.2) 535.8 - 1981.4 [260.10 - 3973.79]
Non-DS Subjects	-0.418 (±0.691) -1.423 - 0.720	-0.133(±0.887) -1.218 - 1.500 [-7.313 - 3.384]	1083(±0.482.5) 497.5 - 1873.37 [205.98 - 4386.87]
Eyes Closed	ANDA log K (PP)($1/s^2$)	INDA log K (PP) ($1/s^2$)	K_e (IP) (N*m/rad)
DS Subjects	1.252 (±0.427) 0.472 - 2.070	2.866 (±.926) 1.495 - 4.915 [-0.0624 - 5.455]	1366.9 (±493.3) 584.2 - 1796.8 [420.51 - 5750.55]
Non-DS Subjects	-0.188 (±0.758) -1.323 - 0.805	0.412 (±1.164) -1.739 - 1.928 [-5.564 – 3.628]	976.4 (±587.4) 523.1 - 2437.1 [160.96 - 7926.19]

Table 3.4: Summary statistics for each of the stiffness parameters. The second column shows the average (±SD) and the minimum - maximum values of $\log(K)$ computed by fitting the nonlinear model to the average normalized autocorrelation functions over the ten trials for each subject by condition. The last two columns show the average of the subject averages over trials (±SD of the subject averages over trials) and the minimum - maximum of the subject averages over trial. The last row in each block is the minimum - maximum over all subjects and trials within the category.

approximate, however, and the X's should be used only as a general guide, not to make goodness of fit conclusions about the model.

3.3 The Inverted Pendulum Model

3.3.1 Implementing the IP Model

The IP model requires the estimation of the COM, and the calculation of the COM-COP difference. Recalling (2.25), which stated that $p_y = y - \frac{h_e}{g}\ddot{y}$, we see the relationship between COM, y, and COP, p_y. p_y is estimated from B-splines via standard least squares methods, using a spline-estimated version of the right hand side of (2.25); B-splines to represent time are used in place of y and $\ddot{y}$ as follows:

$$XQ = X - \frac{h}{g}Q \tag{3.9}$$

where X represents the B-spline for y, Q represents the B-spline for $\ddot{y}$, g is the gravitational constant, and h is height for a particular subject. The coefficients from the least-squares linear model fitting p_y as the dependent variable and XQ as the independent variable (using SPLUS function **lm**) are then used to estimate y, the position of the COM. Another SPLUS function, **bs**, is used to produce the B-splines.

When estimating the COM from the COP, choosing the proper dimension for the B-spline basis is critical. Choosing a basis with too few dimensions results in an overly smooth estimate of the COM which will not oscillate about the COP frequently enough. A basis of too many dimensions results in a COM which follows the COP too closely, resulting in too many oscillations in the COM-COP difference. Dimension of the B-splines used for y and $\ddot{y}$

(2.25) are specified as a parameter in the **bs** function. This function is also able to automatically produce the B-spline used in place of $\ddot{y}$, which is the second derivative of the B-spline used in place of y. Selecting the proper dimension for the bases used in the procedure is done to try and simulate the COM-COP relationship as measured directly in Winter et al. (1998). A dimension of 200 was chosen for the estimation procedure. A typical COM-COP plot is shown in Figure 3.2 (subject 19, trial 4).

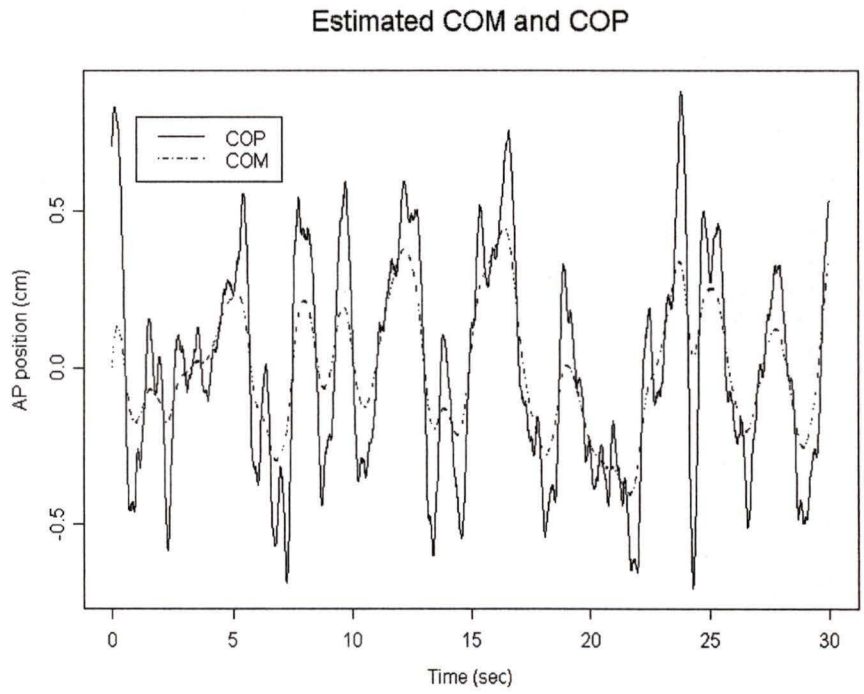

Figure 3.2: The anteposterior component of a Center of Pressure (COP) trajectory and the estimated COM. The large difference seen at the beginning of the trajectory is expected under the estimation procedure.

Because of the estimation procedure, either the beginning or the end (or both) of the estimated COM tends to be poorly estimated. A larger basis dimension reduces this problem somewhat. For further data analysis, however, one or two large differences will not affect the results. Obtaining an estimate for the dominant frequency of the COM-COP difference is of interest, which should not be largely affected by this problem.

Once the COM has been estimated satisfactorily, the COM-COP difference is calculated through subtraction, with resulting estimates of COM-COP appearing as in Figure 3.3.

Once the COM-COP difference has been estimated, frequency analysis is able to proceed. The first step of this procedure is using the SPLUS function **spec.pgram**, which estimates the amplitude spectrum using a discrete Fourier transform. The output from this function gives spectrum results in decibels and frequencies on the range from 0 to π. To remain consistent with Winter et al. (1998), these outputs are transformed so that the spectrum is in centimeters and the frequencies are in Hertz. Once the data are on the proper scales, the model specified by (2.20) can be fit. The fit specified by (2.20) requires the inertia constant I. I is a constant which is different for each subject, and requires the height and mass of a subject for calculation. The calculations are done based on Winter (1981, p. 56). Based on the average relative sizes of various body segments, I is calculated by finding the inertial component from each of the lower leg, the upper leg, and the upper body (torso, head, arms). Movements and therefore inertial values are about the ankle in this model. The inertial contribution of a lower leg (ll), where

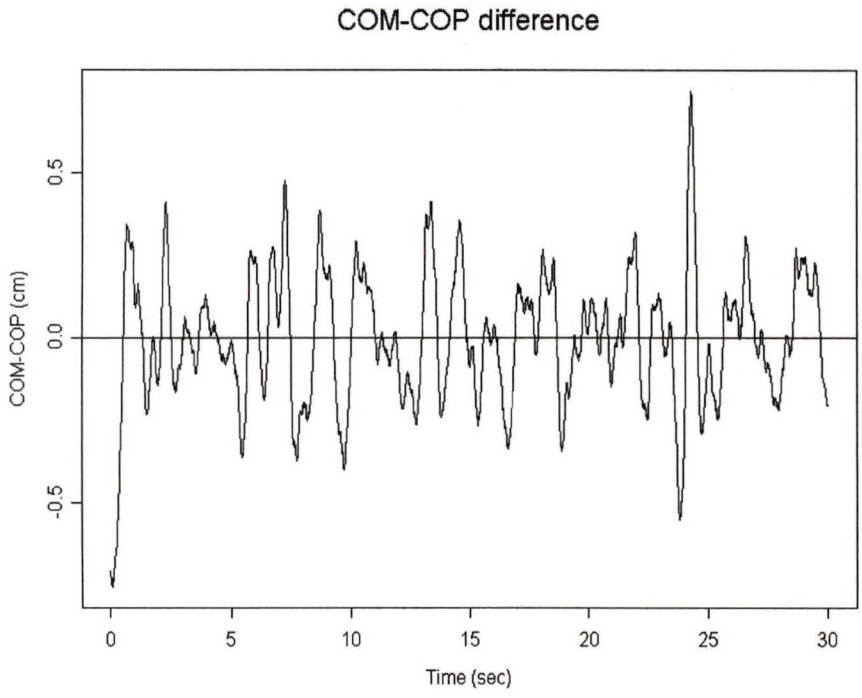

Figure 3.3: The COM-COP difference from the data in Figure 3.2. A large difference is seen at the beginning of the trajectory.

M is the mass and H is the height of a subject, is given as

$$I_{ll} = 0.0463M\left(0.302^2 + (0.567H\left[.285 - .039\right])^2\right), \tag{3.10}$$

the inertia contribution of an upper leg (ul) is given as

$$I_{ul} = 0.1M\left(0.323^2 + (0.567H\left[0.53 - 0.285\right] + H\left[.285 - .039\right])^2\right), \tag{3.11}$$

and the inertial contribution of the upper body (ub) is

$$I_{ub} = 0.678M\left(0.496^2 + (0.626 \times 0.515H + 0.485H)^2\right). \tag{3.12}$$

The overall inertia above the ankle is therefore given by two lower legs, two upper legs, and the upper body,

$$I = 2I_{ll} + 2I_{ul} + I_{ub}. \tag{3.13}$$

No adjustments were made to compensate for differently shaped subjects in terms of the coefficients in the inertial equations. The resulting I values are approximations which likely vary in reliability with the body shape of the subjects. DS subjects do tend to be heavier-set than non-DS subjects, so estimates may be less reliable for the DS subjects. Despite this, it was felt that the estimates were reliable enough to proceed.

The fit to the model in (2.20) was done using a nonlinear fitting algorithm within SPLUS, **nls**. The **nls** function minimizes the sum of the squared residuals through a numerical derivative estimation procedure. B, C, and K_e are the unknown parameters to be estimated (2.20), which stated that $A(\omega) = \frac{C}{\sqrt{1+\left[\frac{I\omega}{B} - \frac{K_e}{\omega B}\right]^2}}$. Initial values need to be assigned to each of the parameters before the start of the optimization algorithm. The procedure is fairly sensitive to these initial values, frequently failing to find a best-fit model on the first attempt. Since trials on the same subject tend to be similar, however, those which fail to fit initially can be redone using initial values from the final fit values of those models which did fit. The final estimates of the

parameters do not change when using different initial values, assuming that the fitting succeeded for all initial values. For 7 out of 377 trials, the fitting algorithm did not converge to a best-fit model for any set of initial values. These trials occurred for both subject groups under both visual conditions; for these trials best-fit solutions can be reasonably estimated by hand through successive parameter selection and plotting of the model with the spectrum.

The final parameter of interest here from the best-fit model is K_e, the effective stiffness of the system with units of Nm/rad. C is a dimensionless scaling constant, and B, the damping constant of the theoretical upright pendulum with units Nms/rad, has a less obvious physical interpretation. The **nls** function provides estimates of all three parameters, as well as residuals. The sum of the squared residuals is used as a measure of the error of the fit to the amplitude spectrum.

3.3.2 Results from the IP Model

Examining the results of the IP model through analysis of K_e estimates, as presented in Table 3.5, shows several significant differences between subject groups and visual conditions, as well as significant trends over trials. In summary, there is a marginally significant trial effect (p=0.053), a significant EO/EC effect (p=0.048), an interaction between subject group and EO/EC condition (p=0.025), and an interaction between trial and EO/EC condition (p=0.035). Figure 3.4 displays these effects where estimated values for K_e under each of the EO/EC and DS versus non-DS conditions are graphed

versus trial number. The K_e estimates for DS subjects are larger under EC versus EO conditions and display a slightly different trend over trial. The K_e estimates for non-DS subjects decrease over trials under the EO condition and increase over trials under the EC condition. The DS estimates are larger than the non-DS estimates under both EO/EC conditions and over all trials.

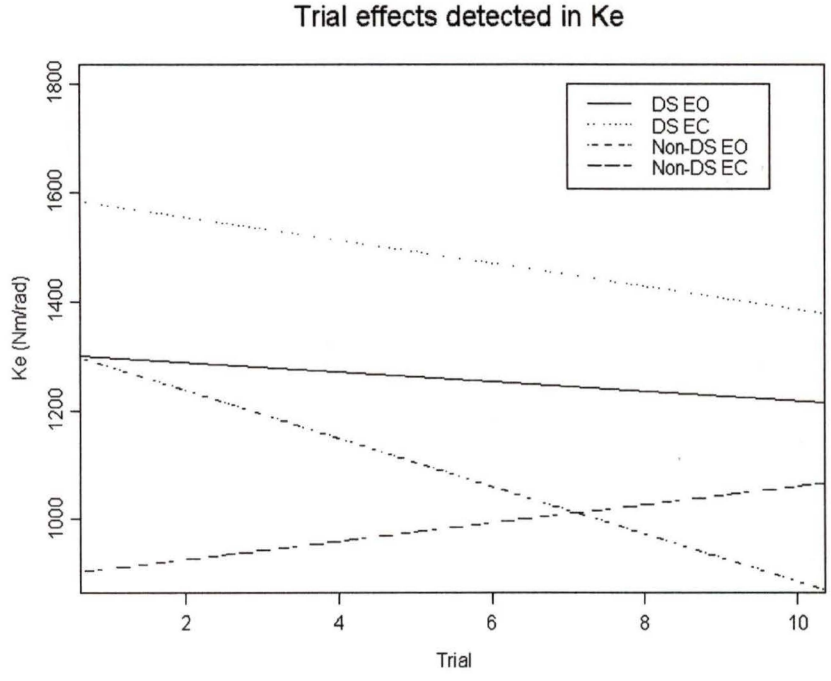

Figure 3.4: GEE model fitting results for K_e. Estimated values for K_e under each of the EO/EC and DS versus non-DS conditions are graphed versus trial number.

The sum of squared residuals on individual trials varied from 0.0000250 to 0.148. Those trials for which fitting a model was most difficult were not

GEE Results	Trial	DS	EO/EC	Trial × DS	Trial × EO/EC	DS × EO/EC	Trial × DS × EO/EC
K_e (IP) (N*m/rad)	**-43.95** **(22.76)** **0.053**	-18.19 (347.06) 0.96	**-434.47** **(219.92)** **0.048**	34.9 (37.27) 0.35	**61.16** **(28.98)** **0.035**	**723.49** **(322.01)** **0.025**	-73.72 (53.09) 0.16

Table 3.5: Results from a GEE model fit of K_e (1^{st} column) versus the independent variables (1^{st} row). Within each cell are the coefficient estimates, the standard error in brackets, and the p-value for testing the hypothesis that the coefficient is zero. Significant or marginally significant p-values appear in bold.

characterized by a higher sum of the square residuals. Those subjects with higher K_e estimates tended to have a greater average squared residual sum, with the maximum occurring at 0.0563 for subject 9 under EC conditions. This subject had the third highest average K_e value and the second highest individual K_e value in the EC condition. The sum of the squared residuals produced by the model fitting procedure do not appear to be informative evaluating the fitted model, as they depend more on the scale of the spectrum than the goodness of fit of the model. A higher K_e value means the spectrum is shifted to higher frequencies and tends to have higher amplitudes as well. This makes sum of squares error terms which are of the same proportion with respect to the data larger in absolute terms.

3.4 FARIMA Models

3.4.1 Implementing the FARIMA model

Implementing the FARIMA model for postural sway, as presented by Sabatini (2000), involves several steps. As shown by Sabatini (2000), the Hurst exponent H, and hence an estimate of $d = H - 1/2$ is calculated without any pre-processsing of the data. Calculations were done to produce the root mean square (RMS) fluctuations as specified by (2.46), in SPLUS. A best-fit line was fit on the log-log scale RMS estimates versus time lags from 1-10 seconds. This line was fit using the **lm** function in SPLUS, which uses standard least-squares regression techniques. The slope of the line is the estimate of H.

Prior to further data analysis, as in Sabatini (2000), "*...the discrete data were prefiltered with a zero-phase 100-point digital FIR filter with corner frequency (-3dB) at 5 Hz and down-sampled by ten...*"(p 1220). In the case of this study, the new time series produced by this procedure will then be 300, instead of 3000, points long. Filters of this type are described in Oppenheim and Schafer (1989). Implementation of a filter meeting the specification listed above was done in MATLAB. The function **filtfilt** performs a zero-phase filtering on a given data set. This function requires the input of filtering coefficients. The MATLAB function **fir1** is able to produce filtering coefficients for a desired number of points and with a given corner frequency once a given window type is selected. The window type selects the nature of the weighting of points in a filter. Common choices include a rectangu-

lar window, which applies equal weights to all points included in filtering the current point, and a Hamming window, which applies greater weight to points near the point currently being filtered (Oppenheim and Schafer, 1989). The corner frequency of a filtering window is the frequency above which the signal will no longer retain its original frequency information. As Sabatini (2000) did not indicate which filtering window was used, the default choice within MATLAB, the Hamming window, was used for this analysis. Once all of the specifications of the filtering procedure had been met, it was carried out, followed by the down-sampling. Down-sampling the filter time series was done by retaining every tenth point in the series; the MATLAB routine **downsample** was used to do this.

Once the data had been filtered and down-sampled, the RMS calculations proceeded for all trials and subjects. Calculations were done on the A/P component of a COP trajectory only, as the PP and IP models used only this component. Calculations were again done within MATLAB; The COP increments were calculated, converted to millimeters (for comparison to Sabatini, 2000), and the RMS values were found. Means and standard deviations were calculated within subject and visual condition. Sabatini (2000) calls this measure, "*the strength of stochastic driving*".

Calculating the DC gain, natural frequency, and damping ratio from the filtered, down-sampled data is a multi-stepped process. The first step was to construct a moving average (MA) operator, as in (2.47), to, "*...remove the fractal component from the input signal, yielding an ARMA signal...*"(Sabatini 2000). This in effect, takes the original system, which was

modelled as FARIMA (p,d,q), and removes the data structures that result from the fractional d component. The MA coefficients up to h_7 were calculated for each trial based on the estimate of the Hurst exponent for that trial, and then applied to the data.

The second step is to identify the best-fit ARMA system. Sabatini (2000) suggested that the ARMA(4,0), or equivalently the AR(4), model best fit their data after a detailed residual analysis. Fitting this model to the data was done using MATLAB function **arburg**, which takes as input a time series and the order of the AR model, and returns a vector of coefficients. These coefficients are a_1 to a_5 in the transfer function

$$H(z) = \frac{\sqrt{e}}{1 + a_2 z^{-1} + a_3 z^{-2} + a_4 z^{-3} + a_5 z^{-4}}, \tag{3.14}$$

where a_1 is always equal to 1. The transfer function specified as in (3.14) is then entered into the MATLAB function **tf**. This function takes the coefficients from a transfer function, either in continuous or discrete time, and puts them in a format that MATLAB is able to use for system identification. The data in this study is in discrete time, both prior to and following down-sampling procedures. Using the output from **tf**, two further functions within MATLAB are able to determine the measures of interest here, DC Gain, Natural Frequency, and Damping Ratio. **dcgain** outputs the DC Gain of the system specified by **tf**. The DC Gain is calculable by setting $z = 1$ in (3.14) as well. The function **damp** takes the system specified by **tf** and returns the natural frequencies and corresponding damping ratios. There

are as many frequencies specified as the order of the system, in this case four. The maximum frequency and its damping ratio were recorded as the summary measures.

3.4.2 Results from the FARIMA model

Results from Sabatini's (2000) paper showed two groups of subjects separated by their Hurst exponent (H) estimates. The first of these groups was characterized by a significant change in H between visual conditions in the A/P direction. The second group had no significant change. These results were not seen among the non-DS subjects in this analysis, though age and gender makeup of the subjects were similar to those in Sabatini (2000). The Hurst exponents are summarized in Table 3.6. Significant differences have been evaluated using two-tailed t-tests in this section, as in Sabatini (2000). Paired t-tests have been used when comparing visual conditions within the same subject group.

No non-DS subject showed a significant difference between the visual conditions with respect to H. Non-DS subjects as a group showed an overall significant difference between EO and EC conditions when comparing the subject means (p=0.032). Two DS subjects did show significant differences between the visual conditions. DS subjects as a group showed a significant difference between the visual conditions (p=0.037). All significant differences between visual conditions had lower H values under the EC condition, similar to those results shown in Sabatini (2000). DS subjects also had significantly

lower H values than non-DS subjects under both EO and EC conditions (p=0.0033 and p=0.0020 respectively). The estimates of H were similar in mean and standard deviation to those seen by Sabatini (2000) for non-DS subjects.

Eyes Open	Hurst exponent	Eyes Closed	Hurst exponent
DS Subjects	0.098 (±0.054) 0.044 – 0.188	DS Subjects	0.055 (±0.046) 0.022 – 0.169
Non-DS Subjects	0.225 (±0.092) 0.078 – 0.366	Non-DS Subjects	0.186 (±0.088) 0.085 – 0.306

Table 3.6: Summary of the Hurst exponent fit to the data in this study. Shown are the mean value ± the standard deviation, as well as the maximum and minimum values.

The COP "increments", or the results of taking the first time difference of a filtered, down-sampled COP trajectory, were shown to be non-normal in distribution through the χ^2 and Kolmogorov-Smirnov goodness of fit tests. P-values were less than 0.01 for both versions of this test for all COP increment time series tested. This agrees with the results from Sabatini (2000) which showed the increments were better fit by a Lévy stable distribution with parameter α of about 1.7. The Normal distribution is a special case of the Lévy distribution with $\alpha = 2$. The distribution of the COP increments has heavier tails than a Normal distribution.

The "strength of stochastic driving" (RMS) estimates in the A/P direction are summarized below in Table 3.5. 14 of 18 subjects showed a significant increase (p-value less than 0.1 using a paired t-test) in this measure in the EC condition as compared to the EO condition. Two subjects showed a sig-

nificant decrease, one in each subject group. Non-DS subjects as a group showed no significant difference between the visual conditions (p=0.120). Removing the one subject with a significant increase, however, lowers the p-value to 0.0232. DS subjects also showed no significant difference between visual conditions (p=0.174), although there is a significant difference when the one DS subject who showed a significant increase is removed (p=0.011). The non-DS subjects had estimates of RMS that were in the range of those reported in Sabatini (2000), although all subjects in that paper showed significant increases in the RMS estimates. DS subjects had significantly different RMS measures than non-DS in the EC condition (p=0.019) and in the EO condition (p=0.056). In both cases, DS subjects had the higher estimates. RMS measures for both groups and visual conditions had higher standard deviations than those observed in Sabatini (2000).

Eyes Open	RMS (mm)	Eyes Closed	RMS (mm)
DS Subjects	1.425 (±0.667) 0.506 – 2.340	DS Subjects	1.808 (±0.893) 0.845 – 3.795
Non-DS Subjects	0.808 (±0.273) 0.251 - 1.176	Non-DS Subjects	1.031 (±0.215) 0.703 – 1.361

Table 3.7: Summary of the RMS values in the A/P direction for both groups and visual conditions. Shown are the mean value ± the standard deviation, as well as the maximum and minimum values.

Three further measures were taken on each trial once the AR(4) system was estimated, DC gain, natural frequency, and damping ratio. These are summarized below in Table 3.8.

DC gain values are not of the same order as those obtained by Sabatini

(2000). The reasons for this are unknown, as no indication is given in Sabatini (2000) as to the method used in calculating DC gain, natural frequency, or damping ratio. As compared to the results from Sabatini (2000), those in this study tended to have a higher coefficient of variation (CV; the standard deviation divided by the mean).

Comparing the significant changes observed in the DC gain estimates in this study to those in Sabatini (2000), Sabatini (2000) showed that 6 of 10 subjects showed a significant increase in DC Gain in the EC condition as compared to the EO condition. Only 2 of 9 non-DS subjects in this study showed such an increase, with 4 of 9 showing an increase overall. Subject 5 (non-DS) had very high DC gain results in the EO condition (average DC Gain at 5154), although not in the EC condition. Reasons for this are unknown, and the other two measures extracted in the same procedure seemed to be reasonable. Very high DC Gain measures were also observed for two DS subjects, subject 13 in the EO condition (average 1545) and subject 14 (average 1720) in the EC condition. For the same subjects, results from the other visual condition appeared to be consistent with the rest of the results.

Overall, DS subjects showed a significant decrease in DC gain in the EC condition ($p=0.021$), with only subject 14 (who as mentioned gave odd values in the EC condition) showing an increase. 7 of the 8 observed decreases were significant as well. The non-DS groups showed no significant difference between visual conditions, $p=0.717$. Comparing subject groups by visual condition, the non-DS group is significantly higher in both the EO condition ($p=0.009$) and in the EC condition ($p=0.0023$). The subjects mentioned

above with extreme values for DC gain were removed from the tests.

Eyes Open	DC Gain	Natural Frequency (Hz)	Damping Ratio
DS Subjects	68.95 (±26.96) 20.67 – 218.50	2.012 (±0.379) 1.485 – 2.633	0.424 (±0.134) 0.236 – 0.661
Non-DS Subjects	143.85 (±67.69) 77.14 – 230.59	2.076 (±0.629) 1.705 – 3.526	0.436 (±0.091) 0.344 – 0.639
Eyes Closed	DC Gain	Natural Frequency (Hz)	Damping Ratio
DS Subjects	37.23 (±11.39) 12.60- 77.33	2.065 (±0.606) 1.598 – 3.336	0.387 (±0.081) 0.226 – 0.529
Non-DS Subjects	155.77 (±61.12) 82.69 – 227.84	2.119 (±0.898) 1.512 – 4.434	0.433 (±0.092) 0.281 – 0.555

Table 3.8: Summary of the system summary values in the anteposterior direction for both groups and visual conditions. Shown are the mean value ± the standard deviation, as well as the maximum and minimum values. From the DC Gain measures subjects 5 (non-DS), 13 and 14 (DS) are excluded due to extreme values.

The Natural Frequencies (NF) of the estimated systems follow a similar pattern as those reported in Sabatini (2000). Of the 9 non-DS subjects, 3 show a significant difference in the NF under the EC condition as characterized by a decrease; Sabatini (2000) had 3 of 10 subjects showing a significant decrease in this measure. In this study, one non-DS subject showed a significant increase in the NF under the EC condition. No significant increases were reported by Sabatini (2000), although a similar proportion of increases were observed (3 out of 10 in Sabatini (2000) versus 4 out of 9 in this study). 4 of 9 DS subjects showed significant differences between visual conditions, of which two were decreases and two were increases.

There were no significant differences between subject groups and/or visual condition, with all 4 sub-groupings of results showing similar ranges and means. The estimates of the NF values were more than twice as large as those in Sabatini (2000). The cause of this difference is unknown. The NF estimates all remained under 5 Hz (above which the filtering procedure should have removed), although some did approach that level. CV values tended to be higher in this study than those reported by Sabatini (2000).

The estimates of damping ratio in this study came closest in magnitude amongst the three system measures to those reported by Sabatini (2000). Two subjects showed a significant difference between the visual conditions. One non-DS subject showed a significant increase in the EC condition, and one DS subject showed a significant decrease in the EC condition. 10 of 18 (5 non-DS, 5 DS) subjects showed a decrease in damping ratio in the EC condition, which seems to differ from the 3 of 10 subjects in Sabatini (2000). The estimates of the damping ratios were slightly smaller in this study as compared to Sabatini (2000).

There were no significant differences between subject groups and/or visual condition, with all 4 sub-groupings of results showing similar ranges and means. The CV's, unlike the other measures discussed here, were smaller for damping ratio than those in Sabatini (2000).

Chapter 4

Discussion

4.1 DS versus non-DS Results

The original purpose of implementing the PP and IP models was to evaluate physical properties of Down syndrome subjects as compared to non-DS subjects. Previous studies (Vuillerme et al., 2001, Vieregge et al., 1996, Shumway-Cook and Woollacott, 1985) have shown DS subjects have a higher COP velocity at various stages of development. The underlying physiological reason for the increase in velocity is less clear. A higher COP velocity is typically associated with greater stiffness, but passive measures of muscle tone show DS subjects to be characterized by hypotonia, or low muscle tone.

By analyzing the dynamics of COP data through the PP and IP models, specific parameters, i.e., postural stiffness, can be extracted that relate more directly to the behaviour of the neuromuscular system. The results from this study have provided some insights into the nature of the control systems

underlying postural control in individuals with DS. Individuals with DS have higher estimated values of postural stiffness (for both models) than non-DS subjects. While muscle activity was not measured directly in this study, there have been reports in the literature demonstrating a pattern of muscle co-contraction in DS subjects. Latash (2000) has suggested that individuals with DS may be more likely to use co-contraction strategies that optimize safety and stability, particularly in situations where unexpected perturbations are likely to occur. As this strategy would also lead to an increase in effective stiffness, it seems a likely explanation of the results seen in this study.

Furthermore, the increase in postural stiffness in the eyes closed condition for individuals with DS may be particularly important. The increase in postural stiffness suggests that individuals with DS do have a certain dependency on visual input and that removal of this input enhances the underlying co-activation strategy.

A third significant finding is the decrease in postural stiffness over trials for DS subjects, as shown by the IP model (but not the PP model). This finding suggests that individuals with DS are able, over time, to modulate their underlying muscle stiffness. If, as suggested by Latash (2000), DS subjects use strategies for tasks that maximize safety, the decrease over trials may suggest that they feel less threatened by a previously unfamiliar task after practice has occurred.

Results from the FARIMA models with respect to DC gain estimates are interesting. Sabatini (2000) hypothesized that an higher DC gain may indicate greater stiffness in the postural system. Should that be true, the

FARIMA results are contradicting results from the IP and PP model. In DC gain, the DS group had estimates significantly lower than those of the non-DS group under both visual conditions. If DC gain is reflecting stiffness, this is opposite to the results from both the IP and PP models. The DS group also showed a significant decrease in DC gain under EC conditions; assuming DC gain is reflecting stiffness, this is again opposite to the IP and PP models. As results from the other two models have clearer interpretations and show many of the same patterns, it is reasonable to hypothesize that DC gain does not provide another stiffness measure. In the estimates of natural frequency and damping ratio, no significant differences were seen between the DS and non-DS groups.

4.2 Individual Models

4.2.1 The Pinned Polymer Model

The Pinned Polymer model, as originally presented by Chow and Collins (1995), is a continuation of the work done on Stabilogram-Diffusion analysis (Collins and De Luca, 1993, Collins and De Luca, 1994). In examining the correlation functions of COP trajectories, it was noted that they took on a particular shape, featuring one or two transitions in slope. Slopes were fit to each of the sections in an observed stabilogram-diffusion plot. The values of these slopes pointed the authors to an examinination of known phenomenon that gave a similar correlation structure. One of these was the movement

of a polymer under certain conditions. The model results, therefore, from an attempt to combine the observed correlation structure of the data with a plausible model of postural control. In this respect in is unlike most other attempts to model upright stance, which usually begin with a physical model (such as the IP model).

There are many reasons why the PP model does show promise in modelling postural control. The model applies to quiet stance conditions as well as postural responses to perturbation, both in theory and practice (Lauk et al., 1998). This property allows for greater flexibility in experimental design.

A physical interpretation of the K estimate that results from estimates of α and β is a positive aspect of the PP model. K is proportional to the stiffness of the system, which is an important physical characteristic of postural control systems. Experiments where a non-DS subject artificially stiffened their muscles resulted in values for K that were much higher than those observed under quiet stance for that subject, or for any non-DS subject. These results appear to show that K was providing an estimate of muscle stiffness, at least in some cases.

The PP model does not place limits on the number of points where balancing corrections can be made. This feature is both positive and negative. It does allow for the multi-segmented nature of the body, where movements and postural corrections can occur in the ankles, knees, hips, and upper body. It also does not require that a set of joints (i.e. ankles, knees) act in unison. There are an infinite number of flex points allowed in the model, however, which does not seem a more reasonable approximation to body structure

than a low number of flex points. The PP model does not compensate for physical differences between subjects, as no physical information is required to implement it.

The pinning in the model keeps the COP fluctuating around a fixed location in quiet stance. This implies that the postural systems are always attempting to return to the same point of balance. Observed data does not support this assumption; many COP trajectories show a long-term drift. That is, COP trajectories are quite often non-stationary in the sense that the postural fluctuations are taking place around different locations over time. The PP model is dependent on the structure of the autocorrelation function, in particular the model requires the ACF to drop down fairly quickly, and then fluctuate about zero. Data sets which are non-stationary tend to show a long-term drop-off toward zero, but for many of the data sets under examination, the drop-off to zero and subsequent fluctuations do not occur until well past the time lag chosen as the cutoff for examination, as one would expect for non-stationary data sets.

Implementation of the PP model can be quite challenging, requiring a great deal of programming. This may be what has stopped it from being widely implemented on COP data from various subject groups. Lauk et al. (1999) presented the only implementation in the literature of the PP model to a particular subject group, in that case those with Parkinson's Disease. Particular values of K were not presented in that paper, or in any of the other papers on this topic. This presents another challenge to those wishing to implement the PP model, as there are no results for comparison in the

literature.

4.2.2 The Inverted Pendulum Model

The Inverted Pendulum model, as presented here, was originally proposed by Winter et al. (1998), with continuing work by Morasso and Schieppati (1999). These papers present a method for arriving at a stiffness estimate for the postural control system. They present several important results, including a method for COM estimation and showing that the inverted pendulum system can be stabilized by a proportional + derivative feedback linear controller. This model was apparently constructed starting with the proposed physical representation, with parameters extracted from the natural behaviour of this model.

Represented by a relatively simple physical system, the IP model is able to reproduce many of the structures of the data, such as the close relationship between the COP and the COM. This relationship, measured directly in Winter et al. (1998), is inevitable given the physical model, indicating that the true properties of postural control and the IP model show significant overlap. Another benefit of the IP model is that physical properties of subjects (height, weight) are incorporated directly into the model and calculations.

Estimates of parameters, most importantly the stiffness estimate K_e in this case, are simple to arrive at using standard methods once the COM movements have been collected, or estimated. When estimation of the COM is needed, this is the most difficult and time consuming part of the data

analysis. Estimation of the COM as presented by Morasso et al. (1999) requires the correctness of the IP model as presented there. Using the model to arrive at an estimate for the COM and then using these estimates to analyse the model seems odd, though, and it would be preferable to collect the COM separately, as in Winter et al. (1998). This is costly, however, so it cannot be as widely implemented as a procedure needing only COP collection. The interpretability of K_e as the stiffness of the postural system is a positive aspect of the IP model. This stiffness measure follows from a natural physical property of the system, i.e. the stiffness at the ankle. The model has not been implemented on a subject group such as those with Down syndrome previously.

The IP model is extremely restrictive on the model of the body, allowing movement only at the ankle. This requirement for the model will not be met by all subjects. Specific instructions to move only at the ankle would make natural quiet stance difficult, however, even for those subjects who naturally move predominantly at the ankle joint.

The IP model is not dependent upon the COP trajectory being stationary. The model can be applied no matter the behaviour of the COP, as the COM-COP difference does not depend on the data remaining in any one area. For this reason, perhaps this model could be extended to perturbed postural behaviour as well. This would require that a subject react to a perturbation with changes at the ankles, however, which may not be a reasonable expectation in such a situation.

4.2.3 FARIMA Models

FARIMA models attempt to explain the structures observed within COP data, similar to the PP model. FARIMA models for COP data, as implemented by Sabatini (2000), are able to explain the behaviour of the the stabilogram-diffusion plots (as in Figure 2.2), "*...without resorting to the controversial hypothesis of the open-loop/closed-loop control mechanism*" (Sabatini, 2000, p. 1225). The structures seen in the stabilogram-diffusion plots are natural to a system resulting from a FARIMA(p,d,q) model where $d \neq 0$. The short-term correlation structure can be seen as resulting not from a postural control system characteristic, but rather from the collection and processing of data from a FARIMA system of this type.

Being a statistical model rather than a physical one does have some advantages. By selecting a FARIMA framework, analysis of the model can utilize pre-existing methods without the need to derive properties beforehand. This is seen in Sabatini (2000), where estimates of FARIMA parameters p, d and q are found, followed by a summary of the resulting system through the DC gain, natural frequency, and damping ratio. Implementing a similar analysis requires no programming of model-specific functions, and is able to proceed using pre-existing functions within MATLAB, or equivalent signal processing software as well.

Removing COP data from a physical model entirely makes it more difficult than in the PP and IP models (see Figures 2.3 and 2.6) to visualize what is happening in the system in clearly interpretable terms. Observations

about the estimates of DC gain, natural frequency, and damping ratio can be said to be consistent with physical interpretations, but do not themselves represent meaningful physical properties, at least in terms of a person. This also means, however, that interpretations of parameter estimates are not limited by a physical model. That said, an estimable parameter with direct physical interpretations is of greater use to clinicians and others who may make treatment decisions based upon a COP analysis. That type of measure is not provided by the FARIMA model.

4.3 Summary of Models and Future Research

There is a great deal of overlap between the three main models presented here. The IP and PP models are both estimating the stiffness of the postural control system, even while the physical models corresponding to these two bear little resemblance to one another. K and K_e have a weak positive correlation on a trial-by-trial basis of 0.36, indicating that they may be making measurements on the same property of the postural system. While the correlation is low, both models show a great deal of variability within and between subjects, making a high correlation unlikely. Neither the K or K_e have any notable correlation with the measure of passive muscle tone, as displayed for K in Figure 4.1. There are a low number of passive measures outside the normal category, so the power of these comparisons are greatly limited.

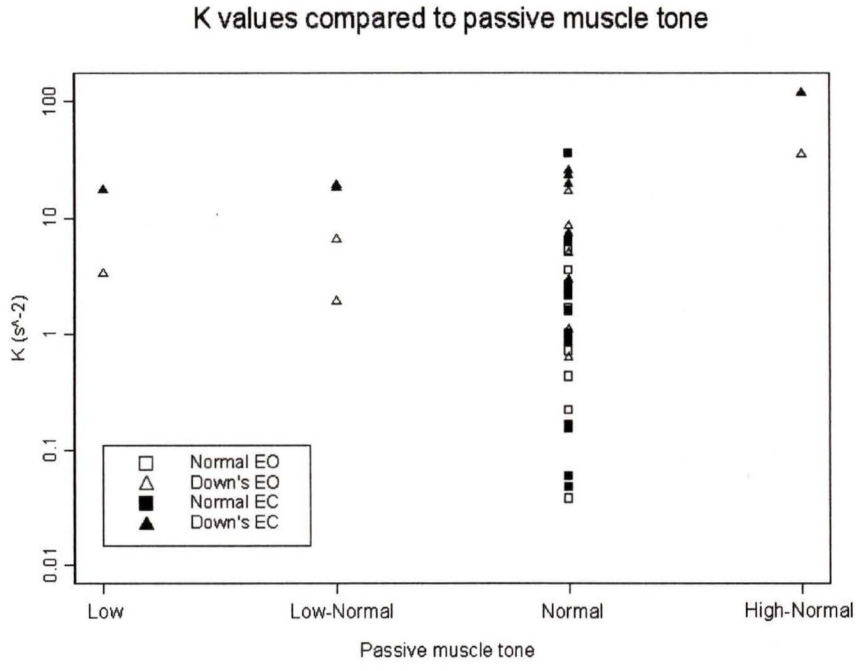

Figure 4.1: The PP model average estimates for individual stiffness versus the clinical passive muscle tone measure. There is no significant relationship between these two measures. Similar results are observed for the IP model.

The FARIMA and IP models are both making measurements in the frequency domain. K_e is equivalent to $I \times \omega_n$ in the IP system, where ω_n is the natural frequency of the system. This makes K_e a very similar measure to the natural frequency in the FARIMA models. The systems being measured, however, are not the same, as the IP model is measuring characteristics of the COM-COP difference, whereas the FARIMA model is measuring characteristics of just the COP data. There is no indication from the estimated

parameters, however, that the two measures are redundant; they appear to be giving different information about the same COP data.

The implementation difficulties encountered in the PP model make it an unlikely choice of model for those without a programming and mathematical background. Fitting the PP model is more complicated than the other methods due to the need to program an optimization procedure such as the L-M method. Finding a best-fit model takes far longer with the PP model, as each trial must be handled separately. The heavy dependence on initial values and their variability makes it impossible to select suitable values without resorting to trial and error for each COP trajectory.

There are several possibilities for improving the PP model. Many problems were encountered in the fitting process which may be attributable to the non-stationarity of COP data. This could be dealt with in two ways. The first is to somehow remove the non-stationarity from the COP data without removing important correlation structures. Should this be done, the PP model would likely fit all of the data better. Secondly, the inherent non-stationarity could be incorporated in to the mathematical model specified by (2.6) by making μ a function of time as well. Mathematically, this would increase the complexity of the system, and the resulting system may not lend itself to a solution such as the Bessel function result in the current system. Another possibility for improvement is to attempt to circumvent the non-stationarity problems by fitting to an INDA or ANDA for only a very short time lag, perhaps < 1 second. At very short time lags, the correlation structure is less affected by the non-stationarity. As this would limit the model fitting

to a very small amount of the correlation structure, longer trials could be collected to increase the reliability of the information contained there.

As implemented in this study, the IP model seems to be the most reliable and interpretable. This model does not suffer from problems with non-stationarity as the PP model does, but still provides the stiffness measure K_e which may be of clinical usefulness, unlike the FARIMA model. The use of subject measures such as height and weight which are not incorporated into the other models is also a positive, making the model resemble the true physical situation more. The IP model did not fit all of the data (7 of 377 data sets failed to fit), and requires either the use of B-splines to estimate the COM, or the extra expense of collecting the COM simultaneously with the COP. The use of spline estimation is ideal if the model accurately reflects the true physical systems, but may be prone to errors when a subject deviates from this model.

Improvements can be made to the IP model as well. The physical model could be altered in many ways. It could allow the ankles to move in ways other than in complete unison. Hip and knee movements could also be included in the physical model. These changes would make the physics of the model far more difficult, but may be useful in better approximating the true systems. From an experimental standpoint, subjects could be asked to make balance adjustments only at the ankles. Movements collected under such conditions should fit the IP model very well. This would pose problems, however, for groups with pre-existing balance problems. This includes most of the groups usually studied, such as those with DS, Parkinson's disease, or

the elderly.

The FARIMA model is the easiest to implement from raw COP data, requiring only access to MATLAB or other signal processing software that is capable of performing the same tasks. Results do not have the natural interpretability of the IP and PP models, which is a major drawback. The similarity of the measures of the IP and FARIMA models do suggest that perhaps the FARIMA model could be linked to a physical model; this should provide estimated characteristics of the system with a physical meaning that can be related directly to the postural control system.

Quiet stance is a mostly subconscious activity, and apparently corrections to the postural system are made, at least in part, in an anticipatory manner to correct for present and possible future problems. This makes the characteristics of the feedback system difficult to isolate. This contrasts with tasks which give similar data, such as following a moving image with a finger (Beuter et al., 1993). In such tasks, reaction times and feedback delays are easier to measure as the tasks take conscious control. In postural control, three systems (Visual, Somatosensory, Vestibular) constantly and interdependently make corrections. Isolating these systems for analysis is very difficult, and doing so can make the balance task itself challenging to a subject. Posing these types of challenges to subjects with pre-existing balance difficulties (such as DS or PD patients) may be unwise. For instance, confusing the vestibular systems can lead to motion sickness and vertigo.

In conclusion, COP data contains much information beyond that which basic measures such as velocity can tell us. Extracting this information

as physiologically meaningful parameter estimates is an ongoing area of research. All three models covered here in detail show some promise for extracting useful information from COP trajectories, with some promising results having been found already. Both the PP and IP models currently produce stiffness estimates of the postural system, and both models do seem to measure this characteristic with some success. Application of these models to DS subjects has been done for the first time here, yielding possibly important information about them. These models may also serve as a base for future work able to extract more detailed information from COP data.

Chapter 5

References

Bendat JS and Piersol AG (1984) Random Data: Analysis and Measurement Procedures. New York: Wiley, 1984.

Beuter A, Bélair J, Labrie C (1993) Feedback and Delays in Neurological Diseases: A modeling study using dynamical systems. Bulletin of Mathematical Biology 55(3): 525-541

Box GE and Jenkins GM (1976) Time Series Analysis: Forecasting and Control, 2^{nd}edition. Oakland: Holden-Day

Chow CC, Collins JJ (1995) Pinned polymer model of posture control. Physical Review E 52: 907-912

Chow CC, Lauk M, Collins JJ (1999) The dynamics of quasistatic posture control. Human Movement Science 18:725-740

Chu DL, Chan HC, Ho DWC (1998) Regularization of Singular Systems by Derivative and Proportional Output Feedback. Siam J. Matrix Anal. Appl. 19(1): 21-38

Collins JJ and De Luca CJ (1993) Open-loop and closed-loop control of posture: A random-walk analysis of center-of-pressure

trajectories. Exp Brain Res 95: 308-318

Collins JJ and De Luca CJ (1994) Random Walking during Quiet Standing. Physical Review Letters 73: 764-767

Collins JJ and De Luca CJ (1994) The effects of visual input on open-loop and closed-loop postural control mechanisms. Experimental Brain Research 103: 151-163

D'Agostino RB, Chase W, Belanger A (1988) The appropriateness of some common procedures for testing the equality of two independent binomial populations. American Statistician 41: 198-202

Deriche M and Tewfik AH (1993) Signal modeling with filtered discrete fractional noise processes. IEEE Trans. Signal Processing, 41: 2839–2849

Després C, Lamoureux D, Beuter A (2000) Standardization of a Neuromotor Test Battery: The CATSYS System. Neurotoxicology 21(5):725-736

Diener HC, Dichgans J, Bacher M, Gompf B (1984) Quantification of Postural Sway in Normals and Patients with Cerebellar Diseases. Electroencephalography and Clinical Neurophysiology 57: 134-142

Diggle PJ, Liang K, Zeger SL (1999) Analysis of Longitudinal data. Great Britain: Oxford University Press

Flugge-Lotz I, Taylor C (1956) Synthesis of a nonlinear control system. IRE Transactions on Automatic Control 1(1): 3-9

Hale FJ (1988) Introduction to Control System Analysis and Design. New Jersey: Prentice Hall

Hosking JRM (1981) Fractional Differencing. Biometrika 68(1): 165-176

Hunter, MC and Hoffman MA (2001) Postural control: visual and cognitive manipulations. Gait and Posture 13: 41-48

Latash ML (2000). Motor coordination in Down Syndrome: The role of adaptive changes. In: Weeks, D.J., Chua, R., Elliott, D (Eds), Perceptual-Motor Behavior in Down Syndrome (199-223). Champaign, IL: Human Kinetics

Lauk M, Chow CC, Lipsitz LA, Mitchell SA, Collins JJ (1999) Assessing muscle stiffness from quiet stance in Parkinson's disease. Muscle Nerve 22: 635-639

Lauk M, Chow CC, Pavlik AE, Collins JJ (1998) Human Balance out of Equilibrium: Nonequilibrium Statistical Mechanics in Posture Control. Physical Review Letters 80(2): 413-416

MacNab YC and Dean CB (2001) Autoregressive Spatial Smoothing and Temporal Spline Smoothing for Mapping Rates. Biometrics 57:949-956

Mandelbrot BB (1968) Fractional Brownian motions, fractional noises and applications. SIAM Rev 10: 422-437

Marsden JE (1973) Basic Complex Analysis. New York: W.H. Freeman and Company

Maylor EA and Wing AM (1996) Age Differences in Postural Stability are Increased by Additional Cognitive Demands. Journal of Gerontology 51B(3): 143-154

Melzer I, Benjuya N, Kaplanski J (2001) Age-related changes of postural control: effect of cognitive tasks. Gerontology 47(4): 189-94

Morasso PG and Schieppati M (1999) Can muscle stiffness alone stabilize upright standing? J Neurophysiol. 83: 1622-1626

Mutambara AGO (1999) Design and Analysis of Control Systems. Unites States of America: CRC Press

Nardone A, Galante M, Lucas B, Schieppati M (2001) Stance control is not affected by paresis and reflex hyperexcitability: the case of spastic patients. J Neurol Nerosurg Psychiatry 70(5): 635-643

Oppenheim AV and Schafer RW (1989) Discrete-time Signal Processing. New Jersey: Prentice Hall

Peng CK, Buldyrev SV, Goldberger AL, Havlin S, Sciortino F, Simons M, Stanley HE (1993) Long-range correlations in nucleotide sequences. Nature 356: 168-170

Press W, Flannery B, Teukolsky S, Vetterling W (1990) Numerical Recipes The Art of Scientific Computing (FORTRAN Version). United States of America: Cambridge University Press

Rencher AC (1995) Methods of Multivariate Analysis. Canada: Wiley- Interscience

SAS Release 8.00, SAS Institute, 1999

Sabatini, AM (2000) A Statistical Mechanical Analysis of Postural Sway Using Non-Gaussian FARIMA Stochastic Models. IEEE Transactions on Biomedical Engineering 47: 1219-1227

Shumway-Cook A and Woollacott MH (1985) Dynamics of postural control in the child with Down Syndrome. Physical Therapy 65(9)

Shumway-Cook A, Anson D, Haller S (1988) Postural Sway Biofeedback: Its Effect on Reestablishing Stance Stability in Hemi-

plegic Patients. Arch Phys Med Rehabil 69: 395-400

Shumway-Cook A and Woollacott MH (2000) Motor Control: Theory and Practical Applications. Lippincott Williams and Wilkins

S-PLUS 6.1 Professional Edition Release 1, Insightful Corp., 2002

Vieregge P, Schulze-Rava H, Wessel K (1996) Quantifaction of Postural Sway in Adult Down's Syndrome. Dev Brain Dysfunct 9:211-214

Viitasalo MK, Kampman V, Sotaniemi KA, Leppävuori S, Myllylä VV, Korpelainen JT (2002) Analysis of Sway in Parkinson's Disease Using a New Inclinometry-Based Method. Movement Disorders 17(4): 663-669

Vuillerme N, Marin L, Debû B (2001). Assessment of static postural control in teenagers with Down Syndrome. APAQ 18: 417-433

Winter, D. A. Biomechanics and Motor Control of Human Movement (2^{nd} ed.) (1990). New York

Winter DA, Patla AE, Prince F, Ishac M, Gielo-Perczak K (1998) Stiffness control of balance in quiet standing. J Neurophysiol. 80: 1211-1221

Appendix A

Commands and Code

A.1 Introduction to notation

We use the following naming conventions for COP trajectories: *subject*000**COP, where *subject* is the abbreviation for a subject, for instance NVB for subject 8, or DR for subject 1 (see masterdata.xls). An example is the first EC COP trajectory for subject 7 is denoted BM00002COP, the last EC COP trajectory BM00011COP. ** represents the TRAJECTORYNUMBER. All trajectory numbers run from 02 to 21, except for subject 8 (NVB), wh0 has 2-11, and 14-23 (because of poorly collected trials). Subject 9 (JF) is missing 11, and subject 3 (MA) is missing 10 due to problems with data collection.

Heights are abbreviated h*subject,* i.e. hAA, hDR.

Masses are abbreviated m*subject*, i.e. mAA, mDR.

Inertias are abbreviated I*subject,* i.e. IA, IDR.

Note that lower or uppercase letters may be used sometimes for the *subject*, i.e. MA or ma, NVB or nvb.

The estimated COM for a particular COP trajectory is denoted COM*subjectTRAJECTORYNUMBER*, i.e., the first EO COM trajectory for subject 7 is called COMBM02, the first EC COM COMBM12.

Naming conventions are similar for the COM-COP differences, i.e. COM-COPBM12.

The code below takes an exported COP trajectory for the AMTI software, centres it at (0,0), and converts it to centimetres from the inches it exports as. Change BQ to any other abbreviation for a subject for any of the trials. Change the number of the trial to run it for any particular trial for a subject.

```
BQ00002COP[,1]<-BQ00002COP[,1]*2.54- mean(BQ00002COP[,1]) *2.54
```

A.2 Descriptive Measures

The various descriptive measures were not calculated, instead taken directly from the AMTI software after accuracy was confirmed using SPLUS.

The following code was run in SAS to obtain the output for the GEE models in Chapter 3. The data set 'alldata' contains columns for each measure on the subject for each trial, including subject number, all four descriptive measures, the values of a DS indicator variable, an EO/EC indicator, a trial variable, as well as K and K_e values and transformed values. The procedure **genmod** is called with, in this case, the measure x-range as the dependent variable. Other sub-commands in **genmod** were chosen to fit well to the data. The repeated step 'subject=subject' tells the procedure that multiple measurements were made on the same subjects.

```
proc genmod data=alldata ;
class subject Downs_0 EO_1;
model Xrange = time Downs_0 EO_1 Downs_0*time Downs_0*EO_1 EO_1*time
EO_1*time*Downs_0 / dist=nor
link=identity;
repeated subject=subject / type=exch covb ;
run;
```

To run the GEE models for the other descriptive measures, as well as K

and K_e, simply replace 'model Xrange' with any other variable, i.e. 'model Yrange' or 'model K'.

A.3 SPLUS functions

This section lists all of the functions that were written to analyze COP data in the PP model and the IP model. Function names are in boldface. Comments about each function appear above the function itself in italics. These functions are used in the function calls of later sections in this appendix. Functions to do with implementing the PP model fitting via Levenburg-Marquardt method are based on those in Press et al. (1990).

This function is one of the approximations for the L-M method, in this case it is for the first order Bessel function with an imaginary root. Used for the PP model.

```
Bessl1 <- function(x)
{
x <- sqrt(x 2.)
p1 <- 0.5
p2 <- 0.87890594
p3 <- 0.51498869
p4 <- 0.15084934
p5 <- 0.02658733
p6 <- 0.00301532
p7 <- 0.00032411
q1 <- 0.39894228
q2 <- -0.02282967
q3 <- -0.00362018
q4 <- 0.00163801
q5 <- -0.01031555
```

```
q6 <- 0.02282967
q7 <- -0.02895312
q8 <- 0.01787654
q9 <- -0.00420059
if(sqrt(x) < 3.75) {
y <- x/14.0625
Bessl1 <- (p1 + y * (p2 + y * (p3 + y * (p4 + y * (p5 + y * (p6 + y *
p7))))))
}
if(sqrt(x) > 3.75) {
AX <- sqrt(x)
y <- 3.75/sqrt(x)
Bessl1 <- (exp(AX)/sqrt(AX)) * (q1 + y * (q2 + y * (q3 + y * (q4 + y *
(q5 + y * (q6 + y * (q7 + y * (q8 + y * q9))))))))
}
Bessl1
}
```

This function is one of the approximations for the L-M method, in this case it is for the zeroth-order Bessel function with an imaginary root. The input is the value 'x', and the output is the Bessel Function value at that value. Used for the PP model.

```
Besslo <- function(x)
{
x <- sqrt(x 2.)
p1 <- 1.
p2 <- 3.5156229
p3 <- 3.0899424
p4 <- 1.2067492
p5 <- 0.2659732
```

```
p6 <- 0.0360768
p7 <- 0.0044813
q1 <- 0.39894228
q2 <- 0.01328592
q3 <- 0.00225319
q4 <- -0.00157565
q5 <- 0.00916281
q6 <- -0.02957706
q7 <- 0.02635537
q8 <- -0.01647633
q9 <- 0.00392377
if(sqrt(x) < 3.75) {
y <- x/14.0625
Besslo <- (p1 + y * (p2 + y * (p3 + y * (p4 + y * (p5 + y * (p6 + y *
p7))))))
}
if(sqrt(x) > 3.75) {
AX <- sqrt(x)
y <- 3.75/sqrt(x)
Besslo <- (exp(AX)/sqrt(AX)) * (q1 + y * (q2 + y * (q3 + y * (q4 + y *
(q5 + y * (q6 + y * (q7 + y * (q8 + y * q9))))))))
}
Besslo
}
```

This function is one of the approximations for the L-M method, in this case it is for the first order Bessel function with a real valued root. The input is the value 'x', and the output is the Bessel Function value at that value. Used for the PP model.

BessJ1<- function(x)

```
    {
    r1 <- 72362614232.
    r2 <- -7895059235.
    r3 <- 242395853.1
    r4 <- -2972611.439
    r5 <- 15704.4826
    r6 <- -30.16036606
    s1 <- 144725228442.
    s2 <- 2300535178.
    s3 <- 18583304.74
    s4 <- 99447.43394
    s5 <- 376.9991397
    s6 <- 1.
    p1 <- 1.
    p2 <- 0.00183105
    p3 <- -3.516396496e-005
    p4 <- 2.457520174e-006
    p5 <- -2.4033719e-007
    q1 <- 0.04687499995
    q2 <- -0.0002002690873
    q3 <- 8.449199096e-006
    q4 <- -8.8228987e-007
    q5 <- 1.05787412e-007
    if(x <= 8.) {
    y <- x 2.
    BessJ1 <- (x * (r1 + y * (r2 + y * (r3 + y * (r4 + y * (r5 + y * r6))))))/(s1
+ y * (s2 + y * (s3 + y * (s4 + y * (s5 + y * s6)))))
    }
    if(x > 8.) {
```

z <- 8./x

y <- z 2.

XX <- x - 2.356194491

BessJ1 <- sqrt(0.636619772/x) * (cos(XX) * (p1 + y * (p2 + y * (p3 + y * (p4 + y * p5)))) - z * sin(XX) * (q1 + y * (q2 + y * (q3 + y * (q4 + y * q5)))))

}

BessJ1

}

This function is one of the approximations for the L-M method, in this case it is for the zeroth-order Bessel function with an real valued root. The input is the value 'x', and the output is the Bessel Function value at that value. Used for the PP model.

BessJo <- function(x)

{

r1 <- 57568490574.

r2 <- -13362590354.

r3 <- 651619640.

r4 <- -11214424.18

r5 <- 77392.33017

r6 <- -184.9052456

s1 <- 57568490411.

s2 <- 1029532985.

s3 <- 9494680.718

s4 <- 59272.64583

s5 <- 267.8532712

s6 <- 1.

q1 <- -0.01562499995

q2 <- 0.0001430488765

```
q3 <- -6.911147651e-006
q4 <- 7.621095161e-007
q5 <- -9.34945152e-008
p1 <- 1.
p2 <- -0.00109862862
p3 <- 2.734510407e-005
p4 <- -2.073370639e-006
p5 <- -6.911147651e-006
if(x > 0. && x <= 8.) {
y <- x 2.
bj <- (r1 + y * (r2 + y * (r3 + y * (r4 + y * (r5 + y * r6)))))/(s1 + y *
(s2 + y * (s3 + y * (s4 + y * (s5 + y * s6)))))
}
if(x > 8.) {
z <- 8./x
y <- z 2.
XX <- x - 0.785398164
bj <- sqrt(0.636619772/x) * (cos(XX) * (p1 + y * (p2 + y * (p3 + y * (p4
+ y * p5)))) - z * sin(XX) * (q1 + y * (q2 + y * (q3 + y * (q4 + y * q5)))))
}
BessJo <- bj
BessJo
}
```

This function calculates the value of the cost function in the L-M method. It is not used within the L-M method routines, but can be used separately from the main routines when evaluating a model or double checking a fit, which resembles a Chi-square statistic. Used for the PP model.

```
chisqfit <-function(fittedmodel, normave, sdave, maxlag)
{
```

```
fitchi <- 0.
for(i in 2.:600.) {
fitchi <- fitchi + ((normave[i] - fittedmodel[i])/sdave[i]) 2.
}
chisqfit <- fitchi
chisqfit
}
```

This function takes the input values of the time-point (from zero to nine seconds), and the current values of alpha and beta in the optimization routines, and returns the value of the derivative of the Bessel function as in (??) taken with respect to alpha, except in this case it is for the zeroth order Bessel function with an imaginary input value. Used for the PP model.

```
dRdaIo<- function(timepoint, alpha, beta)
{
dRdaIo <- - BessI1((timepoint * timepoint * (4. * alpha * beta - 1.))/(4.
* beta * beta)) * (timepoint/(sqrt((4. * alpha * beta - 1.) 2.))) * exp( -
timepoint/(2. * beta))
}
```

This function takes the input values of the time-point (from zero to nine seconds), and the current values of alpha and beta in the optimization routines, and returns the value of the derivative of the Bessel function as in (??) taken with respect to alpha, except in this case it is for the zeroth order Bessel function with a real valued input. Used for the PP model.

```
dRdaJo <-function(timepoint, alpha, beta)
{
dRdaJo <- - BessJ1((timepoint * sqrt(4. * alpha * beta - 1.))/(2. * beta))
* (timepoint/(sqrt(4. * alpha * beta - 1.))) * exp( - timepoint/(2. * beta))
}
```

This function takes the input values of the time-point (from zero to nine

seconds), and the current values of alpha and beta in the optimization routines, and returns the value of the derivative of the Bessel function as in (??) taken with respect to beta, except in this case it is for the zeroth order Bessel function with an imaginary input. Used for the PP model.

dRdbIo <- function(timepoint, alpha, beta)

{

dRdbIo <- (timepoint/(2. * beta * beta)) * BessIo((timepoint * timepoint * (4. * alpha * beta - 1.))/(4. * beta * beta)) * exp(- timepoint/(2. * beta)) - (exp(- timepoint/(2. * beta)) * BessI1((timepoint * timepoint * (4. * alpha * beta - 1.))/(4. * beta * beta)) * timepoint * (-2. * alpha * beta + 1.))/(2. * beta * beta * sqrt(((4. * alpha * beta - 1.) 2.) 0.5))

}

This function takes the input values of the time-point (from zero to six seconds), and the current values of alpha and beta in the optimization routines, and returns the value of the derivative of the Bessel function as in (??) taken with respect to beta, except in this case it is for the zeroth order Bessel function with a real valued input. Used for the PP model.

dRdbJo<- function(timepoint, alpha, beta)

{

dRdbJo <- (timepoint/(2. * beta * beta)) * BessJo((timepoint * sqrt(4. * alpha * beta - 1.))/(2. * beta)) * exp(- timepoint/(2. * beta)) - (exp(- timepoint/(2. * beta)) * BessJ1((timepoint * sqrt(4. * alpha * beta - 1.))/(2. * beta)) * timepoint * (-2. * alpha * beta + 1.))/(2. * beta * beta * sqrt(4. * alpha * beta - 1.))

}

This function takes the input values of the time-point (from zero to six seconds), the current values of alpha and beta in the optimization routines, and the input 'maxlag', which specifies the number of points to fit in the model. In this study, maxlag=600, specifying a model fit to the first six

seconds of the data. This function returns the model that the L-M method has specified. This function is used when plotting the data, as well as selecting initial values for a good fit to the data. Used for the PP model.

fittedmodel<- function(alpha, beta, timeindex, maxlag)

```
{
fittedmodel <- rep(0., maxlag)
for(i in 1.:maxlag) {
if(4. * alpha * beta > 1.) {
fittedmodel[i] <- exp( - timeindex[i]/(2. * beta)) * BessJo((timeindex[i] *
sqrt(4. * alpha * beta - 1.))/(2. * beta))
}
if(4. * alpha * beta < 1.) {
fittedmodel[i] <- exp( - timeindex[i]/(2. * beta)) * Besslo((timeindex[i] *
timeindex[i] * (4. * alpha * beta - 1.))/(4. * beta * beta))
}
if(4. * alpha * beta == 1.) {
fittedmodel[i] <- 0.5
}
}
fittedmodel
}
```

This function is a useful routine I have implemented in SPLUS, as SPLUS does not have a function (that I could locate), that will return the location of the maximum value in a vector of numbers. This function takes a vector 'x' as input, finds the maximum value and its location, and returns the location of this maximum. It is used to locate the normalization point in the PP data processing steps. Used for the PP model.

maxlocate<-function(x)

```
{
```

```
for(i in 1.:length(x)) {
if(x[i] == max(x)) {
maxlocate <- i
}
}
maxlocate
}
```

This function is one of two main routines, along with 'MRQMIN', which implement the L-M method. It is based on the function of the same name as presented in Press et al. (1990). Based on the input of the INDA or ANDA in the vector 'data', and its standard deviation in 'stdevdata', as well as the current value of alpha and beta and the 'timeindex' of interest, this function calculates the variance matrices used in minimization. Used for the PP model.

```
MRQCOF<- function(timeindex, data, stdevdata, alpha, beta)
{
CHISQ <- 0.
OMEGA <- matrix(0., 2., 2.)
ADAM <- c(0., 0.)
derivalpha <- 0.
derivbeta <- 0.
WTalpha <- 0.
DY <- 0.
Wtbeta <- 0.
fitmodel <- fittedmodel(alpha, beta, timeindex, length(data))
SIG2I <- 1./(stdevdata 2.)
for(i in 1.:length(data)) {
if(4. * alpha * beta >= 1.) {
derivalpha[i] <- dRdaJo(timeindex[i], alpha, beta)
```

```
derivbeta[i] <- dRdbJo(timeindex[i], alpha, beta)
}
if(4. * alpha * beta < 1.) {
derivalpha[i] <- dRdaIo(timeindex[i], alpha, beta)
derivbeta[i] <- dRdbIo(timeindex[i], alpha, beta)
}
DY[i] <- data[i] - fitmodel[i]
WTalpha[i] <- derivalpha[i] * SIG2I[i]
WTbeta[i] <- derivbeta[i] * SIG2I[i]
OMEGA[1., 1.] <- OMEGA[1., 1.] + WTalpha[i] * derivalpha[i]
OMEGA[2., 1.] <- OMEGA[2., 1.] + WTbeta[i] * derivalpha[i]
OMEGA[2., 2.] <- OMEGA[2., 2.] + WTbeta[i] * derivbeta[i]
ADAM[1.] <- ADAM[1.] + DY[i] * WTalpha[i]
ADAM[2.] <- ADAM[2.] + DY[i] * WTbeta[i]
CHISQ <- CHISQ + DY[i] * DY[i] * SIG2I[i]
}
OMEGA[1., 2.] <- OMEGA[2., 1.]
c(CHISQ, OMEGA, ADAM)
}
```

This function is one of two main routines, along with 'MRQCOF', which implement the L-M method. It is based on the function of the same name as presented in Press et al. (1990). Based on the output of MRQCOF (called within this function), it determines the new attempt at a best-fit model, and then determines whether or not the new model is better and should be retained based on a chi-square based statistic. Used for the PP model.

MRQMIN<-function(timeindex, data, stdevdata, alpha, beta, alamda, OMEGA, ADAM, OCHISQ)

```
{
if(alamda < 0.) {
```

```
alamda <- 0.001
temp <- MRQCOF(timeindex, data, stdevdata, alpha, beta)
OCHISQ <- temp[1.]
OMEGA[1., 1.] <- temp[2.]
OMEGA[2., 1.] <- temp[3.]
OMEGA[1., 2.] <- temp[4.]
OMEGA[2., 2.] <- temp[5.]
ADAM[1.] <- temp[6.]
ADAM[2.] <- temp[7.]
}
ALPHAtry <- alpha
BETAtry <- beta
for(j in 1.:2.) {
for(k in 1.:2.) {
COVAR[j, k] <- OMEGA[j, k]
}
COVAR[j, j] <- OMEGA[j, j] * (1. + alamda)
DA[j] <- ADAM[j]
}
DA <- solve(COVAR, DA)
COVAR <- solve(COVAR)
ALPHAtry <- ALPHAtry + DA[1.]
BETAtry <- BETAtry + DA[2.]
if(ALPHAtry > 0. && BETAtry > 0.) {
temp <- MRQCOF(timeindex, data, stdevdata, ALPHAtry, BETAtry)
CHISQ <- temp[1.]
}
if(ALPHAtry < 0. || BETAtry < 0.) {
CHISQ <- 100000.
```

```
}
if(CHISQ < OCHISQ) {
alamda <- alamda * 0.1
OCHISQ <- CHISQ
OMEGA <- COVAR
ADAM <- DA
alpha <- ALPHAtry
beta <- BETAtry
}
if(CHISQ > OCHISQ) {
alamda <- alamda * 10.
CHISQ <- OCHISQ
}
c(alpha, beta, alamda, CHISQ, OMEGA, ADAM)
}
```

*This function is the main data processing function for the PP model. It takes as input the A/P component of ten COP trajectories and the value of maxlag. Within the function, 1.5*maxlag is used; this is done so once the maximum point normalization procedure is done, there will almost always 6 seconds of data left. In a few cases, the normalization point occurred later than 3 seconds, meaning that to analyse those COP trajectories, maxlag had to be increased. Similar functions were created to analyse 2 to 10 COP trajectories in this manner; as they are entirely repetitive, they have been omitted. See comments inside the function as well, indicated by % at the beginning of the line. Output is an ANDA and it's standard deviation.*

normsdave10<-function(y1, y2, y3, y4, y5, y6, y7, y8, y9, y10, maxlag)

```
{
%Get the autocorrelation values for each of the COP trajectories
```

```
y1acf <- acf(y1, 1.5 * maxlag, plot = F)$acf
y2acf <- acf(y2, 1.5 * maxlag, plot = F)$acf
y3acf <- acf(y3, 1.5 * maxlag, plot = F)$acf
y4acf <- acf(y4, 1.5 * maxlag, plot = F)$acf
y5acf <- acf(y5, 1.5 * maxlag, plot = F)$acf
y6acf <- acf(y6, 1.5 * maxlag, plot = F)$acf
y7acf <- acf(y7, 1.5 * maxlag, plot = F)$acf
y8acf <- acf(y8, 1.5 * maxlag, plot = F)$acf
y9acf <- acf(y9, 1.5 * maxlag, plot = F)$acf
y10acf <- acf(y10, 1.5 * maxlag, plot = F)$acf
%Get the negative derivative estimate by taking the negative first difference
%of the ACF from above.
y1diff <- y1acf[1.:(1.5 * maxlag)] - y1acf[2.:(1.5 * maxlag + 1.)]
y2diff <- y2acf[1.:(1.5 * maxlag)] - y2acf[2.:(1.5 * maxlag + 1.)]
y3diff <- y3acf[1.:(1.5 * maxlag)] - y3acf[2.:(1.5 * maxlag + 1.)]
y4diff <- y4acf[1.:(1.5 * maxlag)] - y4acf[2.:(1.5 * maxlag + 1.)]
y5diff <- y5acf[1.:(1.5 * maxlag)] - y5acf[2.:(1.5 * maxlag + 1.)]
y6diff <- y6acf[1.:(1.5 * maxlag)] - y6acf[2.:(1.5 * maxlag + 1.)]
y7diff <- y7acf[1.:(1.5 * maxlag)] - y7acf[2.:(1.5 * maxlag + 1.)]
y8diff <- y8acf[1.:(1.5 * maxlag)] - y8acf[2.:(1.5 * maxlag + 1.)]
y9diff <- y9acf[1.:(1.5 * maxlag)] - y9acf[2.:(1.5 * maxlag + 1.)]
y10diff <- y10acf[1.:(1.5 * maxlag)] - y10acf[2.:(1.5 * maxlag + 1.)]
%Find the normalization point
y1max <- maxlocate(y1diff)
y2max <- maxlocate(y2diff)
y3max <- maxlocate(y3diff)
y4max <- maxlocate(y4diff)
y5max <- maxlocate(y5diff)
y6max <- maxlocate(y6diff)
```

```
y7max <- maxlocate(y7diff)
y8max <- maxlocate(y8diff)
y9max <- maxlocate(y9diff)
y10max <- maxlocate(y10diff)
%cutoff the series at the normalization point and divide through by the max-
imum
%value
y1norm <- y1diff[y1max:(y1max + maxlag)]/y1diff[y1max]
y2norm <- y2diff[y2max:(y2max + maxlag)]/y2diff[y2max]
y3norm <- y3diff[y3max:(y3max + maxlag)]/y3diff[y3max]
y4norm <- y4diff[y4max:(y4max + maxlag)]/y4diff[y4max]
y5norm <- y5diff[y5max:(y5max + maxlag)]/y5diff[y5max]
y6norm <- y6diff[y6max:(y6max + maxlag)]/y6diff[y6max]
y7norm <- y7diff[y7max:(y7max + maxlag)]/y7diff[y7max]
y8norm <- y8diff[y8max:(y8max + maxlag)]/y8diff[y8max]
y9norm <- y9diff[y9max:(y9max + maxlag)]/y9diff[y9max]
y10norm <- y10diff[y10max:(y10max + maxlag)]/y10diff[y10max]
%Find the average of the normalized negative derivatives
normave <- (y1norm + y2norm + y3norm + y4norm + y5norm + y6norm
+ y7norm + y8norm + y9norm + y10norm)/10.
%Find the standard deviation. If the user inputs identical series as the first
% two inputs, the function assumes they are all the same and will return a
%value of 1 for all sd's. If not, the sd is calculated. This was done initially
% so as this function could be used to analyse one series simply by inputting
%it ten times, now no longer needed.
sdave <- 0.
if(y1norm[127.] != y2norm[127.]) {
for(i in 1.:length(y1norm)) {
```

```
sdave[i] <- stdev(c(y1norm[i], y2norm[i], y3norm[i], y4norm[i], y5norm[i],
y6norm[i], y7norm[i], y8norm[i], y9norm[i], y10norm[i]))
}
sdave[1.] <- sdave[2.]
}
if(y1norm[127.] == y2norm[127.]) {
sdave <- rep(1., maxlag)
}
normsdave10 <- cbind(normave, sdave)
normsdave10
}
```

This function is the other main data processing function for the PP model. It takes as input the A/P component one COP trajectories and the value of maxlag. It returns the value of the INDA for that cOP trajectory.

```
normsdave1 = function(y1, maxlag)
{
y1acf <- acf(y1, 1.5 * maxlag, plot = F)$acf
y1diff <- y1acf[1.:(1.5 * maxlag)] - y1acf[2.:(1.5 * maxlag + 1.)]
y1max <- maxlocate(y1diff)
y1norm <- y1diff[y1max:(y1max + maxlag)]/y1diff[y1max]
normave <- (y1norm)
sdave <- 0.
sdave <- rep(1., maxlag)
normsdave1 <- cbind(normave, sdave)
normsdave1
}
```

This function takes the input values of the mass (M) and height (H) of a subject and calculates the inertial about the ankle joint, as in equations 3.10 to 3.13. This is for the IP model, all other functions used for that model are

available in SPLUS.

```
Inertia<- function(M, H)
{
Ileg <- 0.0465 * M * (0.302 2 + (0.567 * (0.285 - 0.039) * H) 2)
Ithigh <- 0.1 * M * (0.323 2 + (0.567 * (0.53 - 0.285) * H + (0.285 - 0.039)
* H) 2)
Ihat <- 0.678 * M * (0.496 2 + (0.626 * 0.515 * H + 0.485 * H) 2)
Inertia <- 2 * (Ileg + Ithigh) + Ihat
Inertia
}
```

A.4 PP Model

This section contains the code used for fitting to the Pinned polymer model. Note that almost all of the functions used here (see SPLUS functions section) work in SPLUS 2000 but a few sometimes complain (due to some strange assignment initialization differences) in the latest version of SPLUS 6.1. Comments about each routine and how to use them are in italics.

First use one of the normsdave (*normalize standard deviation average) functions to put the data into the proper form. Normsdave10 will average ten trials before model fitting (create an ANDA), normsdave1 will do the same for one trial (create an INDA). For only one trial, there is no SD estimate at each point, so a value of 1 is filled in at each point.*

$temp < -normsdave10(CZ00002COP[,2], CZ00003COP[,2],$
$CZ00004COP[,2], CZ00005COP[,2], CZ00006COP[,2], CZ00007COP[,2],$
$CZ00008COP[,2], CZ00009COP[,2], CZ00010COP[,2], CZ00011COP[,2], 600)$

$temp < -normsdave10$
$(CZ00012COP[,2], CZ00013COP[,2], CZ00014COP[,2], CZ00015COP[,2],$
$CZ00016COP[,2], CZ00017COP[,2], CZ00018COP[,2], CZ00019COP[,2],$

$CZ00020COP[,2], CZ00021COP[,2], 600)$

```
temp<-normsdave1(dm00008COP[,2],600)
```

Now get the columns of temp into data and stdevdata. Pick initial values and plot to see if they fit well. fitmodel (the function) outputs the model fit by the given parameters. Note the most important thing to fit to is the first dip in the data (if the data has one that is near zero). Also, for clues as what to fit as initial values, see the existing parameter values that have been fit for a subject.

```
data<-temp[,1]
stdevdata<-temp[,2]
alpha<-5.1093736;beta<-0.3686548;
fitmodel<-fittedmodel(alpha,beta,timeindex,maxlag)
plot(data,type="l")
lines(fitmodel)
```

If the fit is appears to be reasonable, then proceed with the optimization. Run the code below all at once. Once the fit it complete, re-plot the data and model and check if it appears to be good. If not, retry the previous step for different initial values until satisfied. Also check the value of ***alamda****; it should have a value of 1 or more (it changes by factors of ten). If* ***alamda*** *is low (0.1 or less), it means the algorithm has just found a better model, and should be run through the loop below again (without the alamda initialization statement at the beginning of the code below).*

```
alamda<–1
temp<-MRQMIN(timeindex,data,stdevdata,alpha, beta,alamda,OMEGA,ADAM,OCHISQ)
alpha<-temp[1]
beta<-temp[2]
alamda<-temp[3]
OCHISQ<- temp[4]
OMEGA<-matrix(temp[5:8],2)
```

```
ADAM<-matrix(temp[9:10])
alpha
beta
for (i in 1:5){
temp<- MRQMIN(timeindex,data,stdevdata,alpha,beta,alamda,OMEGA,ADAM,OCHISQ)
alpha<-temp[1]
beta<-temp[2]
alamda<-temp[3]
OCHISQ<- temp[4]
OMEGA<-matrix(temp[5:8],2)
ADAM<-matrix(temp[9:10])
temp
}
```

Re-plot the model using the following code to decide if the model found is acceptable.

```
fitmodel<-fittedmodel(alpha,beta,timeindex,maxlag)
plot(data,type="l",main="Model fit to ACF derivative",xlab="Time lag",ylab="Normalized
ACF derivative")
lines(fitmodel,type="l",lty=3)
legend(250,.8,c("ACF normalized derivative","Model Fit"),lty=c(1 ,3))
```

*Check the final parameter estimates in "**qwerty**". Keep **qwerty** open and you can copy and paste the results from there to excel or another spreadsheet program.*

```
temp
k<-alpha/beta
qwerty<-cbind(alpha,beta,k,OCHISQ)
```

At the end of these trials, the vector called 'qwerty' contains four estimates of interest, those for alpha, beta, K, and the χ^2 value for the chosen model fit. These can be exported or copied to a new data file in order to

keep track of each trial's best-fit model.

A.5 IP Model

This section contains commands used for data processing, estimation, and model fitting for the IP model. They are used with SPLUS functions listed in Section 2 of this appendix. Also needed are the heights in metres and masses in kilograms of the subjects. Note that SPLUS version 6.1 or better must be used to ensure all the functions used below are available. The function **bs** was not capable of providing derivatives of the B-splines prior to version 6.1 of SPLUS. Comments about sections of code are above them in italics.

The following commands get the B-Spline matrices for later COM estimation

```
X<-bs(timeindex2,200)
Q<-bs(timeindex2,200,derivs=2)
```

The following code must be run for each value of subject*; only the code for two subjects are shown.*

```
XQAS<-X-(hAS/g)*Q
XQDM<-X-(hDM/g)*Q
```

Inertia values about the ankles are necessary for later calculation. These again must be run for each value of subject.

```
IAS<-Inertia(mAS,hAS)
IDM<-Inertia(mDM,hDM)
```

Estimating the COM-COP differences is done using the code below for each of the COP trajectories for a subject. The code must be repeated for each value of subject *and TRAJECTORYNUMBER.*

```
fitAS<-lm(AS00002COP[,2]~XQAS-1)
COMAS02<-X%*%fitAS$coefficients
COMCOPAS02<-COMAS02-AS00002COP[,2]
```

This command gets the spectrum estimate for a particular COM-COP

difference. The code must be repeated for each value of subject *and TRAJECTORYNUMBER. The numerical ending on the new temp1 matrix must also be changed to run through the commands.*

```
temp1<-spec.pgram(COMCOPAS02,detrend=F)
```

These commands rescale the above estimates in 'temp1' to reproduce desired scales as seen in Winter et al. (1998). This code must be run for each 'temp' matrix created above, usual from temp1 to temp10.

```
Aw1<-0.01*10 (temp1$spec[1:301]/10)
w1<- 2*pi*100*temp1$freq[1:301]
fitdata1<-as.data.frame(cbind(Aw1,w1))
```

To fit the models to each COM-COP spectrum, changing initial values may be necessary. I suggest looking at those spectrums which did fit and using values similar to those already given as the best fits. Initial values for a a particular subject can be chosen to be close to the subject. Values in the commands below are typical choices. The values used to obtain fits for each subject and trial were not recorded.

To see the parameter estimates from the particular fit below, type "p1" at the command prompt in SPLUS. The output lists three numbers, which are C, B and K_e. B and K_e at the most important to get closer to the true values when attempting to select good initial values.

This command calls the function nls in SPLUS, fitting the estimated spectrum to the equation specified by (2.20).

```
p1<- (nls(fitdata1$Aw1~ C/sqrt(1+( IBM*fitdata1$w1/B-K/(fitdata1$w1*B))
2), data = fitdata1, control=list(maxiter = 1000),start = list(C=.01,B=25,K=315))$parameters)
```

Once the models are fit above, fit again using the same initial values to obtain the error estimates. If the initial values worked once, they will again.

```
error1<-sum((nls(fitdata1$Aw1~ C/sqrt(1+( IBM*fitdata1$w1/B-K/(fitdata1$w1*B))
2), data = fitdata1, control=list(maxiter = 1000),start = list(C=.01,B=25,K=315))$residuals)
2)
```

The code below assumes that one has analysed a set of ten trials at once. To get all of the results for a set of ten trials, open the array "answers", which contains the estimates. The first three columns are labelled as B, C and K_e, the last is the error term.

This code used SPLUS commands links together estimate vectors from a single subject using rbind and cbind

```
Resids<-rbind(error1,error2,error3,error4,
error5,error6,error7,error8,error9,error10)
COMCOPfit10<-rbind(p1,p2,p3,p4,p5,p6,p7,p8,p9,p10)
answers<-cbind(COMCOPfit10,resids)
```

This following code is necessary should a COM-COP spectrum prove particularly difficult to assign initial values that give convergence. Plot the spectrums and the model fit to see how the parameters should be shifted. Aw1 and w1 are output from commands above; to get the right Aw1 and w1, run the code corresponding to the COM-COP spectrum that is proving difficult to fit, thus correctly assigning w1 and Aw1.

This is a typical plot command in SPLUS, using a log-scale on the x-axis

```
plot(w1,Aw1,log='x',type='l',main="Model fit to Frequency Spectrum",ylab="Frequency")
```

The next three commands are guesses at parameter values to be plotted.

```
B<- 89.36565
K<- 1124.068
C<- 0.102628
```

This command plots the spctrum model corresponding to the parameter values assigned above. Remember to change the underlined inertial value to subject currently being examined.

```
lines (w1, C/sqrt(1+( IBM*w1/B-K/(w1*B)) 2),type='l',lty=2)
```

In the end of this code, the v

A.6 FARIMA model

The data analysis in this section follows the steps outlined by Figure 1 in Sabatini (2000). The first step in the FARIMA data analysis is to calculate the Hurst exponents. This is done as described in the main body of the thesis. The code for this procedure, as implemented in SPLUS follows, based on a log-log scale linear regression. The code in this section can be replicated with minor changes to work for all trials, analysis of a single trial is shown.

The function SDF is used to calculate the values of the RMS for each time lag. As suggested in Sabatini (2000), the initial data points are excluded from the analysis. The final points have also been excluded. Only points for which all time lags could be calculated are included in calculations

```
SDF<-function(x){
diff<-matrix(0,1401,1401)
SDF<-0
for(i in 1:1401){
diff[,i]<-x[(100+i):(1500+i)]-x[100:1500]
SDF[i]<-sqrt(mean(diff[,i] 2))
}
SDF
}
```

*The results of this function are utilized by the following code to calculate the estimate of the slope of the SDF over the time lags from 1-10 seconds, as in Sabatini (2000). The vector Hurst*subjectabbreviation *contains the estimates of the Hurst exponent for each trial of a subject.*

```
HurstDR<-0
x<-DR00012COP[,2]
g<-SDF(x)
model<-lm(log(g[100:1000])~log(100:1000/100))
```

```
plot(log(100:1000/100),log(g[100:1000]))
abline(model$coef)
Hurst<-as.vector(model$coef[2])
HurstDR[1]<-Hurst
```

Similar code is run for each trial of a subject under a particular visual condition; the final estimates of the Hurst exponents are in the vector $Hurst\text{subjectabbreviation}(see first section about naming conventions)$.

The next step taken in the data analysis is to filter and downsample the data. This is again described in the main text of the thesis; the code for doing this is presented below. The first step of the process is to filter the data as described by Sabatini (2000). For these purposes, further data analysis takes place in MATLAB. COP trajectories must be transferred to MATLAB from SPLUS to do this; it is possible to export data from SPLUS to a .mat file which is the readable format for MATLAB.

h sets the filter to be used and its scale. The MATLAB function "fir1" is used to make the filtering window to be used later on.

```
h=fir1(100,.1);
```

The next three commands are used for loading the data into the MATLAB system. The location is not applicable for future applications of the code, but the basic format should be OK. All of the Cop trajectories, in .mat format, were put into the directory C:\Documents and Settings\awebber\My Documents, *where the data is all read from. Note the final \ is necessary for MATLAB.*

```
idn='C:\Documents and Settings\awebber\My Documents\';
ifn = 'AA00002COP.mat';
load([idn, ifn])
```

This command converts a COP trajectory into millimetres, as they were in those units in Sabatini (2000).

```
AA00002COP=data*10;
```

The function 'filtfilt' performs zero-phase filtering, as specified by Sabatini (2000).

```
AA2filt=filtfilt(h,1,AA00002COP);
```

The function 'downsample' performs the down-sampling as specified by Sabatini on the filtered data.

```
AA2dsample=downsample(AA2filt,10);
```

The next four commands calculate the Root Mean Square, or strength of stochastic driving, as done in Sabatini, estimates of the COP increment time series. The square roots are taken later. This is performed on the filtered, down-sampled data prior to any applications of MA operations.

```
y=AA2dsample(2:300,2);
y2=AA2dsample(1:299,2);
diff2=y-y2;
rms2=mean(diff2.*diff2)
```

These commands get to the necessary summaries of the RMS estimates to duplicate those which are reported by Sabatini (2000).

```
mean(sqrt([rms2 rms3 rms4 rms5 rms6 rms7 rms8 rms9 rms10 rms11]))
std(sqrt([rms2 rms3 rms4 rms5 rms6 rms7 rms8 rms9 rms10 rms11]))
```

At this point, the data has been filtered and down-sampled, and it remains to complete the steps specified by Sabatini (2000).

To accomplish the "fractional deconvolution" part of the analysis, the trial-by-trial Hurst exponent estimates are used to form a MA operator. The estimates were already in Excel at this point, so Excel was used to calculate the MA coefficients as specified by Equation 2.56 in the thesis. The Excel calculations take an estimate of H, subtract 0.5 to get an estimate of d, and then have the first seven MA exponents calculated via basic spreadsheet operations. Seven coefficients were chosen as it appeared subsequent coefficients were too small to make a significant difference. This leaves, for each individual, a large matrix o values which were then copied and pasted(as plain

text) into MATLAB. A column of semicolons (;) was added to the excel files so the estimates could be entered directly into MATLAB via the following command.

hDR=[0 0 0 0 0 0 0 0 ;

0.53996294 -0.23001853 1 0.23001853 0.141463527 0.083462607 0.059645227 0.046028657 0.037899649 ;

0.397272234 -0.301363883 1 0.301363883 0.196092036 0.111029672 0.077829245 0.059211057 0.048574489 ;

0.443144423 -0.278427788 1 0.278427788 0.177974911 0.10213222 0.072054922 0.055079144 0.045237833 ;

0.396485391 -0.301757305 1 0.301757305 0.196407388 0.111182471 0.077927588 0.05928096 0.048630863 ;

0.325865462 -0.337067269 1 0.337067269 0.225340807 0.124908868 0.086644884 0.065410982 0.053564564 ;

0.125860073 -0.437069964 1 0.437069964 0.314050058 0.163612756 0.109863918 0.080990581 0.06600916 ;

0.54198689 -0.229006555 1 0.229006555 0.140725278 0.083074515 0.059383215 0.045835228 0.037742383 ;

0.878937815 -0.060531093 1 0.060531093 0.032097553 0.020750735 0.015396539 0.012218393 0.010150641 ;

0.892505827 -0.053747086 1 0.053747086 0.028317918 0.018371277 0.013648398 0.01084142 0.009009855 ;

0.517618555 -0.241190722 1 0.241190722 0.149681843 0.087753938 0.062531661 0.048153358 0.039625947 ;

0.534767885 -0.232616058 1 0.232616058 0.143363144 0.08445924 0.060317344 0.046524418 0.038302644 ;

0.622577889 -0.188711056 1 0.188711056 0.112161459 0.067718937 0.048890339 0.038015549 0.031369859 ;

0.133920816 -0.433039592 1 0.433039592 0.31028144 0.162066244 0.108978146

0.080419738 0.065555782 ;

0.500749599 -0.2496252 1 0.2496252 0.155968971 0.091001385 0.064702691 0.04974383 0.040916765 ;

0.440954392 -0.279522804 1 0.279522804 0.178827901 0.102556442 0.072332343 0.055278866 0.045399314 ;

0.471051925 -0.264474038 1 0.264474038 0.167210277 0.096732592 0.068505773 0.052513645 0.043161789 ;

0.357715395 -0.321142303 1 0.321142303 0.212137341 0.118716136 0.08274107 0.062682362 0.051370901 ;

0.482139034 -0.258930483 1 0.258930483 0.162987739 0.094590995 0.067088953 0.051484227 0.042327852 ;

0.539589619 -0.23020519 1 0.23020519 0.14159981 0.083534203 0.059693545 0.046064317 0.037928641 ;

0.203143048 -0.398428476 1 0.398428476 0.278586863 0.148725596 0.101185947 0.075310943 0.061489051];

This matrix was used for all trials for each subject. The "fractional deconvolution" was then applied to the down-sampled and filtered data sets, as named above, as follows:

```
for i = 1:293
ARMADR2(i) = hDR(2,3:9)*DR2dsample(i:(i+6),2);
end
coefsDR2=arburg(ARMADR2,4);
tfDR2=tf([sqrt(exp(1)) 0 0 0 0],coefsDR2,0.1,'variable','z -1');
dcgain(tfDR2);
[wn,Z]=damp(tfDR2);
props(1,:)=[dcgain(tfDR2) wn(4) min(Z)];
```

This code calculates the characteristic transfer function for each trial, and extracts the summary measures DC gain, Frequency, and damping ratio. These are stored in a matrix called "props", which has the columns corre-

sponding to the three estimated parameters and rows corresponding to trial. Where trials were missing, a row of zeroes was entered as a placeholder. The code above is slightly altered to run for each trial, for a total of 20 trials. The matrix "props" was opened within MATLAB, and the results were copied into Excel from there. At this point, all parameters of the systems identified in the data have been estimated as in Sabatini (2000).

VITA

Surname: Webber Given Names: Adam Matthew

Place of Birth: Truro, Nova Scotia, Canada

Educational Institutions Attended:

University of Victoria	2001 to 2003
Dalhousie University	1996 to 2001

Degrees Awarded:

B.Sc. (Honours, Co-op)	Dalhousie University	2001

Honours and Awards:

Natural Sciences and Engineering Research Council of Canada Postgraduate Scholarship	2001-2003
University of Victoria Research Grant	2001-2003
Advanced Systems Institute of BC Scholarship	2001
University Medal in Statistics, Dalhousie University	2001
Bernoulli Award, Dalhousie University	1999

Publications:

J J S Ludbrook, P T Trunog, M V MacNeil, M Lesperance, A Webber, H Joe, H Martins, J Lim (2003) Do Age and Comorbidity Impact Treatment Allocation and Outcomes in Limited Stage Small-Cell Lung Cancer? A Community-Based Population Analysis. Int. J. Radiation Oncology Biol. Phys., Vol. 55, No. 5, pp. 1321–1330

Contributed to *Report of the Sixth PIMS Industrial Problem Solving Workshop, May 27-31, 2002* (not yet published)

Contributed to *Report of the Fifth PIMS Graduate Mathematics Modelling Camp, May 18-23, 2002* (not yet published)

Adam Webber

UNIVERSITY OF VICTORIA PARTIAL COPYRIGHT LICENSE

Modelling and Analysis of Center of Pressure Data

Author 

Adam M. Webber

September 18, 2003